JOURNAL OF GEOPHYSICAL RESEARCH, VOL. 104, NO. C9, PAGES 20,801–20,826, SEPTEMBER 15, 1999

Seasonal water mass distribution in the Indonesian throughflow entering the Indian Ocean

C. Coatanoan,[1,2] N. Metzl,[3] M. Fieux,[4] and B. Coste[1]

Abstract. A multiparametric approach is used to analyze the seasonal properties of water masses in the eastern Indian Ocean. The data were measured during two cruises of the Java Australia Dynamic Experiment (JADE) program carried out during two opposite seasons: August 1989 (SE monsoon) and February-March 1992 (NW monsoon). These cruises took place at the end of a La Niña event and during an El Niño episode, respectively. Seven sources have been identified in the studied region for the 200-800 m layer: the Subtropical Indian Water, the Indian Central Water, the modified Antarctic Intermediate Water, the Indonesian Subsurface Water, the Indonesian Intermediate Water, the Arabian Sea-Persian Gulf Water (AS-PGW), and the Arabian Sea-Red Sea Water (AS-RSW). The selected tracers are potential temperature, salinity and oxygen with mass conservation and positive mixing coefficients as constraints. The analysis indicates the proportion of each water source along the Australia-Bali section and into the Indonesian channels. Although no large changes are observed for Indonesian waters, significant seasonal variations are found for the southern and northern Indian Ocean water. During the NW monsoon, the contribution of the AS-RSW increases at the entrance of the Indonesian archipelago whereas the contribution of the south Indian waters decreases in the northwest Australia basin. In a complementary study, nutrients are introduced into the multiparametric analysis in order to more clearly separate the signature of the north Indian waters (AS-PGW, AS-RSW) and to provide supplementary information on the biological history of the water masses, which is compared to large-scale primary production estimates.

1. Introduction

The flow from the Pacific Ocean through the Indonesian seas marks the only tropical oceanic connection. This Indonesian throughflow is considered to have an important role in the global oceanic circulation [*Gordon*, 1986; *Schmitz*, 1995]. The Indonesian throughflow is driven by a pressure gradient from the Pacific to the Indian Ocean [*Wyrtki*, 1961]. It is characterized by large seasonal variations due to different wind patterns in the two basins, monsoon in the Indian Ocean and trade wind in the western equatorial Pacific [*Bray et al.*, 1996]. The transport of the throughflow, obtained from direct or indirect methods, varies from -2 to 22 Sv (1 Sv = 10^6 m^3 s^{-1}) [*Piola and Gordon*, 1984; *Fine*, 1985; *Fu*, 1986; *Gordon*, 1986; *Masumoto and Yamagata*, 1993; *Fieux et al.*, 1994; *Miyama et al.*, 1995; *Fieux et al.*, 1996a]; extrema correspond to the Java Australia Dynamic Experiment 1989 (JADE 89) (SE monsoon) and JADE 92 (NW monsoon) cruises. The maximum (estimated from models) occurs from austral autumn to austral winter (SE monsoon), and the minimum occurs during the NW monsoon [*Miyama et al.*, 1995]. As a result, the seasonal current reversal, observed in many locations in the Indonesian seas, directly influences the water mass distribution in the Indonesian basins [*Gordon et al.*, 1994] as well as in the Indian Ocean [*Wyrtki*, 1961]. At an interannual timescale, the currents supplying the Indonesian archipelago are also disturbed by the austral oscillations associated with El Niño-La Niña events [*Chiswell et al.*, 1995; *Kindle and Phoebus*, 1995; *Picaut and Delcroix*, 1995; *Wijffels et al.*, 1995; *Meyers*, 1996]. Beyond their influence on the precipitation-evaporation balance, these events, through changes in the western Pacific sea level, can also intervene on the Indo-Pacific transport.

The water masses flowing through the Indonesian seas and reaching the Indian Ocean have their origin mostly in the North Pacific Ocean [*Lukas et al.*, 1991; *Godfrey et al.*, 1993; *Gordon et al.*, 1994]. The water masses crossing the "maritime continent" basins follow two routes, the eastern and western routes [*Wyrtki*, 1961; *Gordon*, 1986; *Lukas et al.*, 1991; *Fine et al.*, 1994; *Miyama et al.*, 1995]. The Lombok Strait, with a sill depth reaching 350 m [*Murray and Arief*, 1988], allows through only upper waters coming from the Makassar Strait, whose surface waters originate from the upper thermocline North Pacific water [*Gordon and Fine*, 1996]. From the Banda Sea, two passages, situated on both sides of Timor island, allow the spreading of the deeper Indonesian waters into the Indian Ocean [*Rochford*, 1966; *Gordon*, 1986; *Wyrtki*, 1971]. Mixing takes place in the different Indonesian basins [*Van Aken et al.*, 1988; *Ffield and Gordon*, 1992, 1996] and strongly modifies the properties of the waters flowing through the Indonesian archipelago. Consequently, the Pacific signature has completely vanished in the water masses when they enter the Indian Ocean, where we can define them as Indonesian waters [*Fieux et al.*, 1996b]. From the south Indian Ocean, the central water and subtropical water, formed at 40°S-45°S and 25°S-35°S, respectively, are found in the northwestern Australian basin [*Wyrtki*, 1971; *Warren*, 1981; *Toole and*

[1]Laboratoire d'Océanographie et de Biogéochimie, CNRS, Marseille, France.

[2]Now at Department of Marine Chemistry and Geochemistry, Woods Hole Oceanographic Institution, Woods Hole, Massachusetts.

[3]Laboratoire de Physique et Chimie Marines, INSU/CNRS, Université Paris 6, Paris

[4]Laboratoire d'Océanographie Dynamique et de Climatologie, CNRS/ORSTOM/UPMC, Université Paris 6, Paris.

Paper number 1999JC900129.
0148-0227/99/1999JC900129$09 00

Warren, 1993]. Deeper, the Antarctic Intermediate Water is characterized by a salinity minimum (around 1000 m) that appears also off the northwestern Australian shelf [*Wyrtki*, 1971]. Originating from the Red Sea [*Rochford*, 1966; *Toole and Warren*, 1993] or from the mixing of the Red Sea and the Persian Gulf Waters [*You and Tomczak*, 1993; *Fieux et al.*, 1994] and from the Arabian Sea, the Northwest Indian Intermediate Water flows eastward along the Sumatra and Java islands before penetrating into the Savu Sea [*Wyrtki*, 1971; *Fieux et al.*, 1996b].

In order to quantify the contribution of the different water masses to the observed data, an optimum multiparametric analysis (OMPA) was developed by *Mackas et al.* [1987] as an extension of the work by *Tomczak* [1981]. The principle of this analysis is based on an inverse method that uses measurements of the concentration of several tracers to determine the proportional mixture of the different source water types that best describes the composition of the water sample [*Mackas et al.*, 1987]. Many applications, at regional or basin scales, have been undertaken in several oceanic regions. Thus *Mackas et al.* [1987] quantify the importance of deep upwelling of California Undercurrent water onto the continental shelf. *Maamaatuaiahutapu et al.* [1992] attempt to visualize the different cores in the Brazil-Malvines confluence, where the water masses mix in a complex structure. At a larger scale, *Hinrichsen and Tomczak* [1993] describe the water mass distribution in the northern Atlantic basin. *Tomczak and Large* [1989] described the mixing between the Indian Central Water and the Australasian Mediterranean Water (also called Banda Sea Water or Indonesian Intermediate Water) in the eastern Indian Ocean. *You and Tomczak* [1993] studied the water masses of the whole Indian Ocean thermocline with the same method. These are mainly stationary situations, which are studied on isopycnal horizons. Recently, *You* [1997] studied the seasonal variations of water masses in the thermocline of the Indian Ocean by using a set of historical data at large scale and defining seasonal sources.

In this paper, we apply the optimum multiparametric analysis at the regional scale, with the aim of detecting the seasonal variation of the water masses in the Indonesian throughflow entering the Indian Ocean. We use a closely spaced series of stations obtained near and within the Indonesian Straits in the framework of the Java Australia Dynamic Experiment conducted during two opposite seasons. The cruises were carried out at the end of a La Niña event and during an El Niño episode, in August 1989 and February 1992, respectively. Therefore the seasonal study realized from this data set can take into account likely interannual effects resulting from these climatic events. In order to more clearly separate the signature of the north Indian waters, the nutrients will be introduced into the multiparametric analysis. An estimate of the effect of biological processes on the water masses will be made by comparison of the biogeochemical results with large-scale primary production estimates.

2. Data

The JADE 89 and JADE 92 cruises, on board the R/V *Marion Dufresne* of the Institut Français pour la Recherche et la Technologie Polaires (IFRTP), were carried out in August 1989 and February-March 1992, respectively, in the eastern part of the Indian Ocean. The JADE 89 cruise took place at the end of a La Niña event. February 1992 corresponded to an El Niño episode. During JADE 89 (corresponding to the SE monsoon), 65 hydrographic stations were occupied, with 18 between Australia and Bali and 21 off the channels (Figure 1). During JADE 92 (corresponding to the NW monsoon), 29 stations were occupied

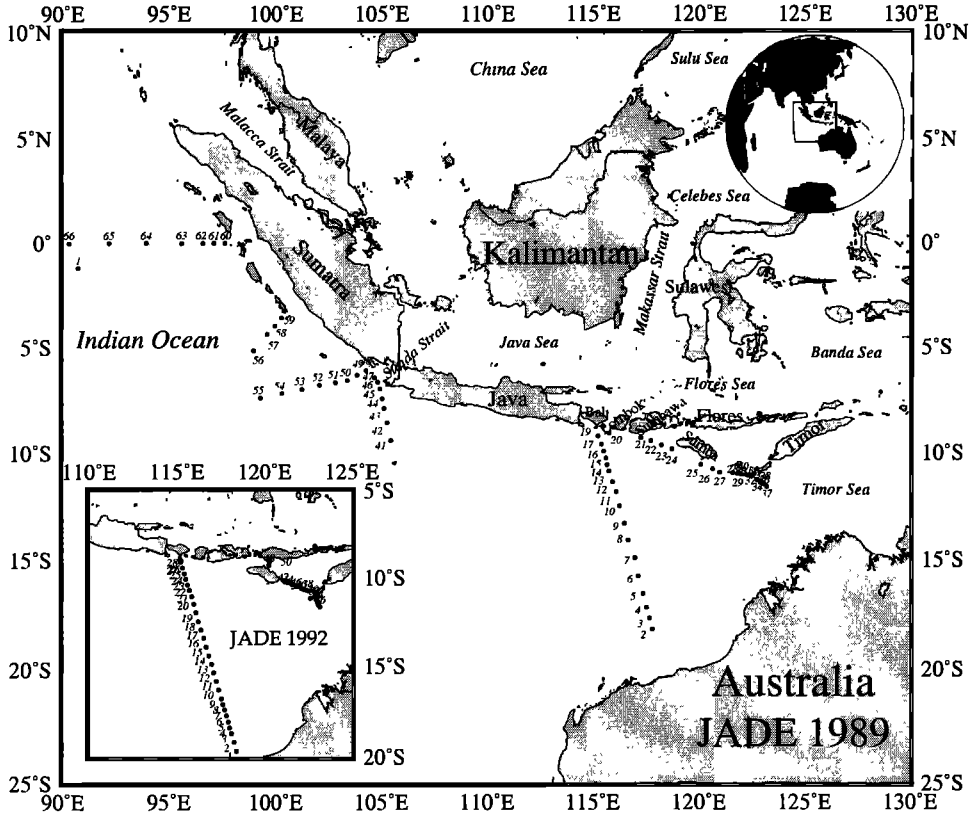

Figure 1. Location of the stations in the two Java Australia Dynamic experiment (JADE) cruises.

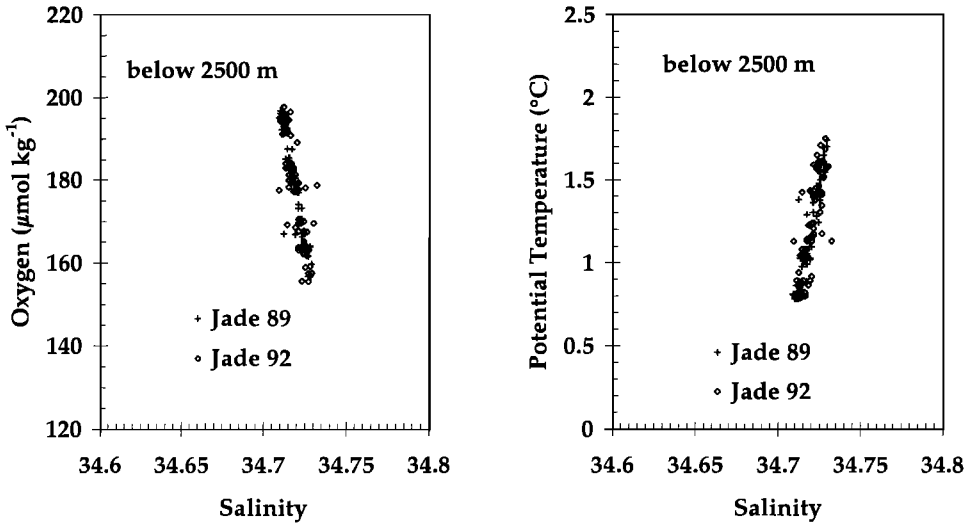

Figure 2. . Comparison of (left) oxygen concentrations (μmol kg^{-1}), (right) potential temperature (°C), and salinity for both cruises below 2500 m.

between Port Hedland (northwest Australia) and Bali (Indonesia). In addition, 21 stations were occupied in the Timor, Roti, Savu, and Sumba Straits. Both sections intersect all the waters carried from the Pacific Ocean through the Indonesian seas toward the Indian Ocean. These channels represent all the possible ways from the Banda Sea toward the Indian Ocean. The conductivity-temperature-depth (CTD) data set from JADE has been discussed by *Fieux et al.* [1994, 1996b]. Nitrate-nitrogen (NO_3), phosphate-phosphorus (PO_4), and silicate-silicon ($Si(OH)_4$) were measured on board during JADE 1989, according to *Treguer and Le Corre* [1975] methodology, with an estimated precision of ±0 1, ±0.02 and ±0.1 μmol kg^{-1}, respectively. Nutrient data are available for JADE 1989 only. In order to test the accuracy of the data obtained during the two seasons, we compared the deep measurements (Figure 2). The average of potential temperature, salinity, and oxygen concentration, below 4000 m in the northwestern Australian basin, are 0.824 ± 0.059°C, 34.712 ± 0.002, and 194.62 ± 1.23 μmol kg^{-1}, respectively, for JADE 1989 and 0 814 ± 0.029°C, 34.712 ± 0.004, and 194.22 ± 1.54 μmol kg^{-1}, respectively, for JADE 1992. Since deep waters are not affected by seasonal (or interannual) variations, the comparison of JADE 1989 and JADE 1992 data suggests that sufficient measurement quality has been achieved for quantifying seasonal variations in the surface and intermediate waters.

3. Method

A water mass is defined as a body of water with a common formation history of all its elements. A given ocean volume can be shared by several such water bodies, which can penetrate each other as a result of mixing [*Tomczak and Large*, 1989]. Mathematically, water masses are described by a relationship describing the different proportions of the various water types and its associated set of standard deviations. Practically, the number of water types (called water sources in our study) for each water mass is finite and small to fully represent a water mass.

For each tracer, the conservation equation can be expressed through the following linear equation·

$$\sum_{i=1}^{n} k_i C_i = C_m \qquad (1)$$

where k_i is the contribution or mixing coefficient of the water source, n is the water source number, C_i is the tracer concentration of the water source i, and C_m is the measured tracer concentration in the seawater sample.

In the seasonal study, all the parameters used are considered to be conservative. In principle, to describe the mixing of n water masses, n-1 conservative tracers are needed. Usually, the two conservative tracers, temperature and salinity, through θ-S diagrams, are used to identify and track water masses. Insofar as geochemical tracers (dissolved oxygen and nutrients) are mathematically independent of temperature and salinity, they can be included in the water mass contribution calculations. Although nonconservative, the geochemical tracers make it possible to get supplementary information on these water masses, taking care that conservation of hydrological tracers (including the continuity equation) is respected. This is generally done by weighting the linear equations with the inverse of the measurement error and checking the residuals of the system after inversion. An alternative approach when using nonconservative tracers consists of taking into account unknowns (ΔNC), which could represent biological processes such as consumption and remineralization [*Bolin et al.*, 1983; *Metzl et al.*, 1989, 1990]. This offers a decoupling between dynamical and biological processes, but at that stage, the unknown represents the total sum of the biological part without differentiation between the sources. When a biological unknown is added, the linear equation (1) is transformed into the following :

$$\sum_{i=1}^{n} k_i NC_i + \Delta NC = NC_m \qquad (2)$$

The linear equation systems (1) and (2) are transformed into the matricial system:

$$\mathbf{M}\,\mathbf{x} = \mathbf{N} \qquad (3)$$

where **M** represents the data vector attached to each coefficient and tracer, **x** is the vector of the coefficients describing the mixing of the sources and **N** corresponds to the data vector of measured tracers in the sample and the values attributed to constraints.

With this method, we use a strict equation to provide mass conservation: $\Sigma x_i = 1$. This equation will be represented in its matricial form and must be exactly satisfied:

$$\mathbf{E}\,\mathbf{x} = \mathbf{f} \quad (4)$$

where **E** is the matrix of order (1, n) with n the number of source water types; **x** is the solution vector (n, 1) giving for each sample the best fitting fractional contribution of each source type. It must minimize the sum of squares of deviation between the measured data and the estimates of model parameters. Here **f** is the vector 1 expressing the condition of mass conservation.

The tracers will obey the conservation equations (1) (and (2) for the nutrients), which are approximately satisfied in a least squares sense. This can be written:

$$\mathbf{A}\,\mathbf{x} \approx \mathbf{b} \quad (5)$$

where **A** is the source definition matrix (p, n) with p tracer values for n source water types; **b** is the column vector (p, 1) with the first p elements equal to the measured concentrations of the tracer variables in a sample that is assumed to be a mixture of the source water types described by **A**.

The convex constraints that express the nonnegativity of the coefficient, $x_i \geq 0$ for all i, are added to the matricial systems (4) and (5):

$$\mathbf{G}\,\mathbf{x} \geq \mathbf{h} \quad (6)$$

where **G** is the unit matrix of order (n, n) and **h** is the null vector (1, n). Such convex constraints will be applied to mixing coefficients as well as to biological unknowns, with negativity constraints for the oxygen and nonnegativity constraints for the nutrients.

The system (4), (5), (6) is normalized and solved with the least squares method with an algorithm of equality and inequality [*Lawson and Hanson*, 1974]. The output vector **x** is the result of the inversion. Its stability is tested by numerical perturbation experiments. They consist of adding random deviations to the measured data (vector **b**) and the elements of the matrix **A**. The absolute values of the imposed deviations are lower than or equal to the estimated standard deviation values of the considered tracer variables. Thirty perturbations give a mean solution vector **x** for each sample. The study of the standard deviations leads to an evaluation of the coefficient validity and to conclude whether or not seasonal variations are significant according to measurement errors and a priori definition of the sources. The system to be solved at each perturbation is :

$$(\mathbf{A} + \Delta\mathbf{A})\,\mathbf{x}' = (\mathbf{b} + \Delta\mathbf{b}) \quad (7)$$

To get information about nonconservative behavior of tracers and possible errors due to the source water types description and uncertainties associated with the measurements, a vector **R** of error on the tracer is calculated. This vector **R** of residuals is the difference between the predicted (**Ax**) and the measured (**b**) data.

This vector is defined by the following matricial system:

$$\mathbf{R} = \mathbf{A}\mathbf{x} - \mathbf{b} \quad (8)$$

with **x** the average of the **x'** obtained from the thirty perturbations.

Thus, in the ideal case, when the source water type descriptions are correct and complete, the measurements are unbiased, and the tracers are conservative, the vector **R** must be zero. The analysis of the spatial distribution of residuals will allow us to select the ocean layers for which origin and mixing of water masses can be discussed according to steady state and tracer conservation assumptions. For this seasonal analysis, only the first 1000 m of the water column will be studied.

4. Water Mass Analysis and Source Characterization

The Australia-Bali section is located at the boundary of water masses from the Indian Ocean and the Indonesian seas. Several data analyses, from the two JADE cruises, were presented by *Fieux et al.* [1994, 1996a, b], *Molcard et al.* [1994, 1996], and C.Coatanoan et al. (Nutrients distribution in the Indonesian straits and along the Sumatra and Java islands during the southern monsoon, submitted to *Oceanologica Acta*, 1997). Previous studies by *Rochford* [1963], *Wyrtki* [1971], *Tomczak and Large* [1989], *You and Tomczak* [1993], and *You* [1997] made it possible to define the water masses mixing in the eastern Indian Ocean basin. Figures 3a-3i illustrate the observed potential temperature, salinity, oxygen, phosphate, nitrate, and silicate distributions along the Australia-Bali section, using only the bottle measurements that correspond to the quantitative analysis applied in this paper and show both seasons side by side.

4.1. Australia-Bali Radial: 0-1000 m Layer

The most pronounced structure, observed during both seasons, is the sharp hydrological front around 13°S-14°S well defined in salinity, oxygen, and nutrients (Figures 3c and 3d). This front reaches the surface during the NW monsoon and is covered by a low-salinity layer during the SE monsoon. South of the front, a salinity maximum (Figures 3c and 3d) is observed above an oxygen maximum (Figures 3e and 3f) associated with minima in nutrients (Figures 3g, 3h, and 3i). The salinity maximum corresponds to the Subtropical Indian Water (STIW) [*Warren*, 1981; *Fieux et al.*, 1994]. Between the two cores of high salinity, a detailed analysis of the hydrology indicates mixing with the lower salinity Indonesian water [*Fieux et al.*, 1994]. During the SE monsoon, the salinity maximum (S>35.1) is associated with minima in phosphate (PO_4<1.20 μmol kg^{-1}), nitrate (NO_3<15 μmol kg^{-1}), and silicate concentrations ($Si(OH)_4$<20 μmol kg^{-1}) (Figure 3i). Deeper, the oxygen maximum defines the Indian Central Water (ICW) [*Warren*, 1981; *Toole and Warren*, 1993; *Fine*, 1993; *Fieux et al.*, 1994], also called Subantarctic Mode Water [*Warren*, 1981]. The northeastward extension of this water mass appears mostly bounded by the hydrological front observed in the Australia-Bali section and limited to the NW Australian basin [*Fieux et al.*, 1994, 1996b]. Like the STIW, the ICW is not homogeneous and separated in two cores, located at 17°30'S and 14°30'S during both seasons. In these cores, the oxygen values are higher at the SE monsoon (O_2>180 μmol kg^{-1}) than at the NW monsoon (O_2>150 μmol kg^{-1}) (Figures 3e and 3f). Low nutrient values (PO_4<1.6 μmol kg^{-1}, NO_3<25 μmol kg^{-1}, and $Si(OH)_4$<30 μmol kg^{-1}) are associated with the oxygen maximum. Between 750 and 1000 m, a salinity minimum (34.58-34.61) has been detected [*Fieux et al.*, 1996b, Figure 3c]. This signal is not apparent in salinity classes chosen here (Figures 3c and 3d). Close to the Australian continental shelf, it could be a faint signature of the Antarctic Intermediate Water (AAIW) influence [*Fieux et al.*, 1994]. In the north, it corresponds to mixing with the Indonesian waters coming particularly from the Timor Passage [*Fieux et al.*, 1996b].

North of the frontal zone, near Bali (Figures 3c and 3e), high salinities (>34.65) and low oxygen concentrations (<90 μmol kg^{-1}) characterize the water masses originating from the North Indian Ocean (as mixing of the Persian Gulf Water (PGW) and the Red Sea Water (RSW) with the Arabian Sea Water). High nutrient values (PO_4>2 μmol kg^{-1}, NO_3>30 μmol kg^{-1} and

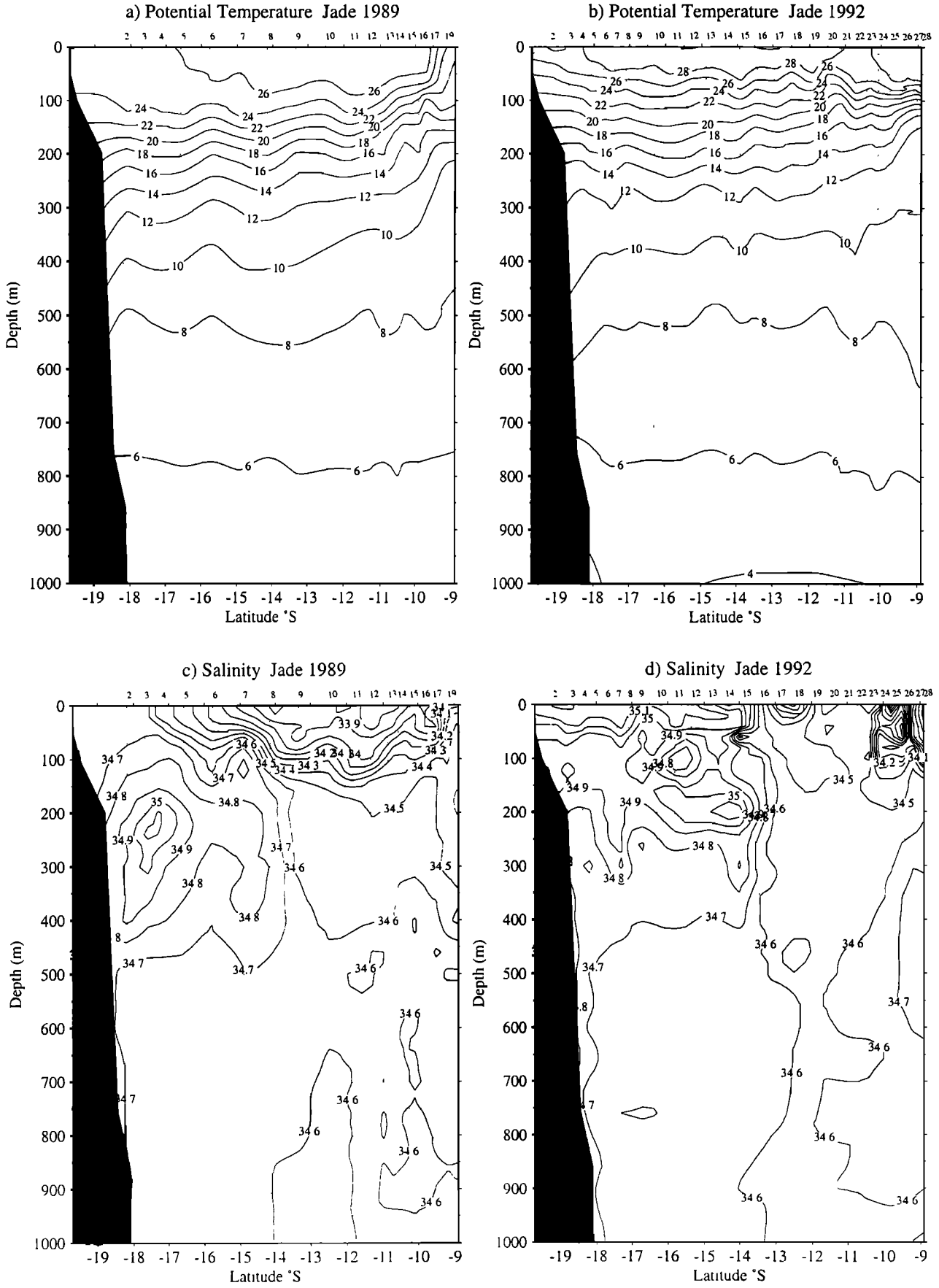

Figure 3. Vertical distribution on the Australia-Bali section of the bottle data for a) potential temperature (°C) Jade 89, b) potential temperature (°C) Jade 92, c) salinity Jade 89, d) salinity Jade 92, e) oxygen (μmol kg^{-1}) Jade 89, f) oxygen (μmol kg^{-1}) Jade 92, g) phosphate (μmol kg^{-1}) Jade 89, h) nitrate (μmol kg^{-1}) Jade 89, i) silicate (μmol kg^{-1}) Jade 89.

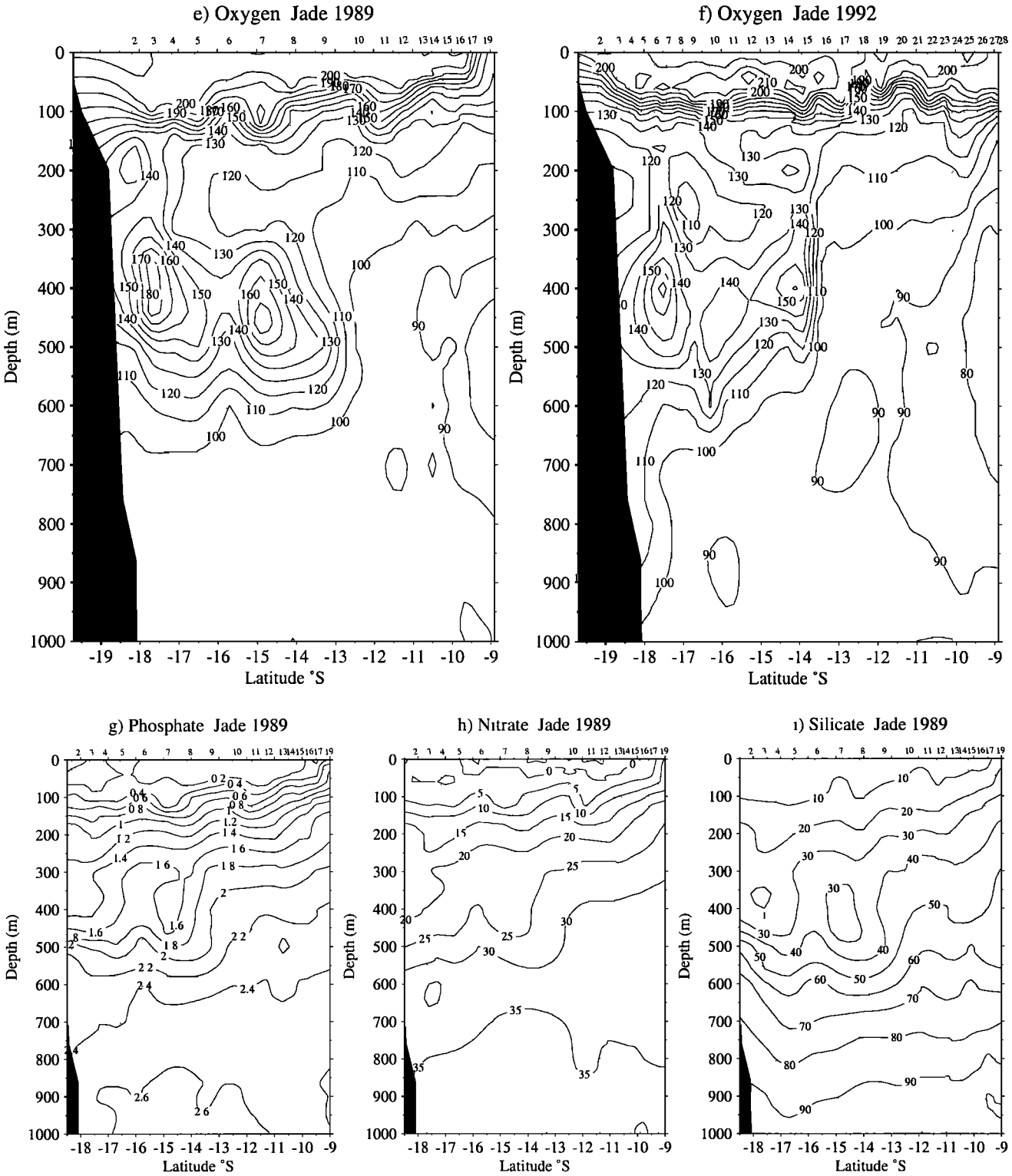

Figure 3. (continued)

$Si(OH)_4$>40 μmol kg^{-1}) are associated with the salinity maximum (Figures 3g, 3h, and 3i). A slight increase of the salinity in Timor Strait could be assigned to a faint influence of this water mass [*Fieux et al.*, 1996b]. Although this water mass has not been previously detected inside the Indonesian archipelago [*Broecker et al.*, 1986; *Van Aken et al.*, 1988; *Van Bennekom*, 1988], it has been shown to enter the Savu Sea [*Fieux et al.*, 1996b].

In the middle of the section, low and homogeneous salinities (Figures 3c and 3d), particularly marked between 13°30'S and 11°S (34.59-34.60), indicate the direct input of the throughflow waters [*Fieux et al.*, 1996b]. The low salinities of Indonesian Subsurface Water (ISW) and the Indonesian Intermediate Water (IIW) at depth, are transported through Timor and Ombai Straits, which draw Indonesian waters from the eastern and western

Table 1a. Data for Water Types of the Australasian Mediterranean Water or Indonesian Water (AAMW), Indian Central Water (ICW), North Indian Central Water (NICW), and Red Sea Water (RSW)

	Potential Temperature, °C	Salinity, psu	Oxygen, μmol kg^{-1}	Phosphate, μmol kg^{-1}	Nitrate, μmol kg^{-1}	Silicate, μmol kg^{-1}	Density, σ_θ
			Tomczak and Large [1989]				
WT1 AAMW	20.00	34.566	124.14	0.810	11.954	7.697	24.4
WT2 AAMW	5.00	34 581	93.50	2.307	37.647	73.906	27.3
WT3 ICW	15.00	35.624	237 78	0.255	0.201	0.754	26.4
WT4 ICW	8.00	34.540	242 85	1.140	17.960	5.353	26.9
			You and Tomczak [1993]				
ICW	18.16	35.624	278.72	0.145	-	2.921	25.7
ICW	9 07	34 805	214.19	1.327	-	10.089	26.9
ICW	4.39	34.384	177 61	1.936	-	43.879	27.3
NICW	15 27	34.840	2.68	2 099	-	25.594	25 7
NICW	7.80	35.098	32 42	2.796	-	60.179	27.3
AAMW	14 89	34.774	112.86	1.615	-	28.638	25.7
AAMW	5.55	34.521	98 61	2.662	-	79 103	27.3
RSW	25.90	38 082	161.90	0.372	-	0.701	25.7

Banda Sea, respectively [*Hautala et al.*, 1996]. This water is relatively rich in silica ($Si(OH)_4$>60 μmol kg^{-1} in the Timor trench [*Van Bennekom*, 1988]). The high percentage of diatoms in the euphotic zone of Indonesian waters involves an important assimilation of dissolved silica in the surface water, especially during the SE monsoon characterized by high productivity in these basins [*Van Bennekom*, 1988] and the sedimentation of the diatom frustules in the water column. Their dissolution leads to a significant silica input into the Indonesian Seas. Consequently, silicate may be an important tracer for separating the various water masses present at the eastern boundary of the Indian Ocean.

4.2. Characterization of Source Waters for the 200-800 m Layer

In the water mass analysis above, excluding the deep waters, we have mentioned source waters with corresponding property extremes: STIW, ICW, modified AAIW (m-AAIW), ISW, IIW, Arabian Sea-PGW (AS-PGW), and Arabian Sea-Red Sea Water (AS-RSW) Considering the core layers of these sources [*Wyrtki*, 1971], the historic data compilation [*Rochford*, 1963; *Tomczak and Large*, 1989; *You and Tomczak*, 1993; *You*, 1997] (Tables 1a and 1b) and the Jade data with their θ-S and θ-O_2 diagrams (Figure 4), we are able to characterize the seven sources (Table 2). For the southern Indian waters, each source will be characterized by an extremum: salinity maximum (35.80) for the Subtropical Indian Water and oxygen maximum (250 μmol kg^{-1}) for the Indian Central Water. A third Indian water mass corresponds to the modified Antarctic Intermediate Water. This water has been defined at a latitude (35°S) where its properties are already modified. For the Indonesian waters, the characterization is given by the diagrams corresponding to the stations occupied in the straits (Figure 5). The Indonesian Subsurface Water and the Indonesian Intermediate Water correspond to the Indonesian water of the upper thermocline and to modified intermediate water of the Banda Sea, respectively, when they enter into the Indian Ocean. For the North Indian Ocean waters, we define two sources from historic data diagrams [*Wyrtki*, 1971]: the Arabian Sea-Persian Gulf Water and the Arabian Sea-Red Sea Water, taking their characteristics in the northwestern and western Arabian Sea, respectively. From the Jade data, a salinity maximum (>35.1 at 250 m near the equator) and a minimum of oxygen (53.6 μmol kg^{-1} observed along the Sumatra and Java coast around 700-800 m) show the presence of both sources along Sumatra and Java. The upper salinity maximum originates from mixing between the Persian Gulf Water entering north of the Arabian Sea and the high-salinity waters typical of the high evaporation observed in the Arabian Sea. Deeper, the salinity maximum characterizes the mixing between the Arabian Sea Water and the Red Sea Water. Their characteristics in this study are taken in the Arabian Sea at 250 m in a region near the output of the Persian Gulf and 600 m near the

Table 1b. Data for Water Types From *You* [1997]

	Potential Temperature, °C		Salinity, psu		Oxygen, μmol kg^{-1}		Phosphate, μmol kg^{-1}		Nitrate, μmol kg^{-1}		Silicate, μmol kg^{-1}		Density, σ_θ
	SW	NE	SW	NE	SW	NE	SW	NE	SW	NE	SW	NE	
ICW	18.15	18 17	35.62	35.62	265 3	260 8	0 06	0.05	-	-	1.57	1.13	25.7
ICW	9 21	9.39	34.79	34.80	225.5	222.4	1.29	1.36	-	-	8.06	8.87	26.9
ICW	6 56	6 77	34.55	34.56	213 9	210.8	1.66	1.76	-	-	21.39	22.49	27.1
NICW	15.60	15.70	34.84	34.85	3 1	1 8	2 13	2.12	-	-	21.44	23.34	25.7
NICW	9.29	9.17	35.05	35 03	23 2	24.1	2.84	2.67	-	-	58.59	58.49	27.1
AAMW	14.96	14 93	34.64	34 63	117 4	117 0	1 41	0.97	-	-	22.94	22.01	25 7
AAMW	14.93	6.90	34.56	34.59	102.7	103 1	2.41	1.78	-	-	80.08	58.67	27.1
RSW	27.60	19 23	39.21	35 97	187.1	74.6	0 12	1 85	-	-	1.07	14.12	25.7

Seasonal variations, according to the SW and NE monsoon, are defined by *You* [1997].

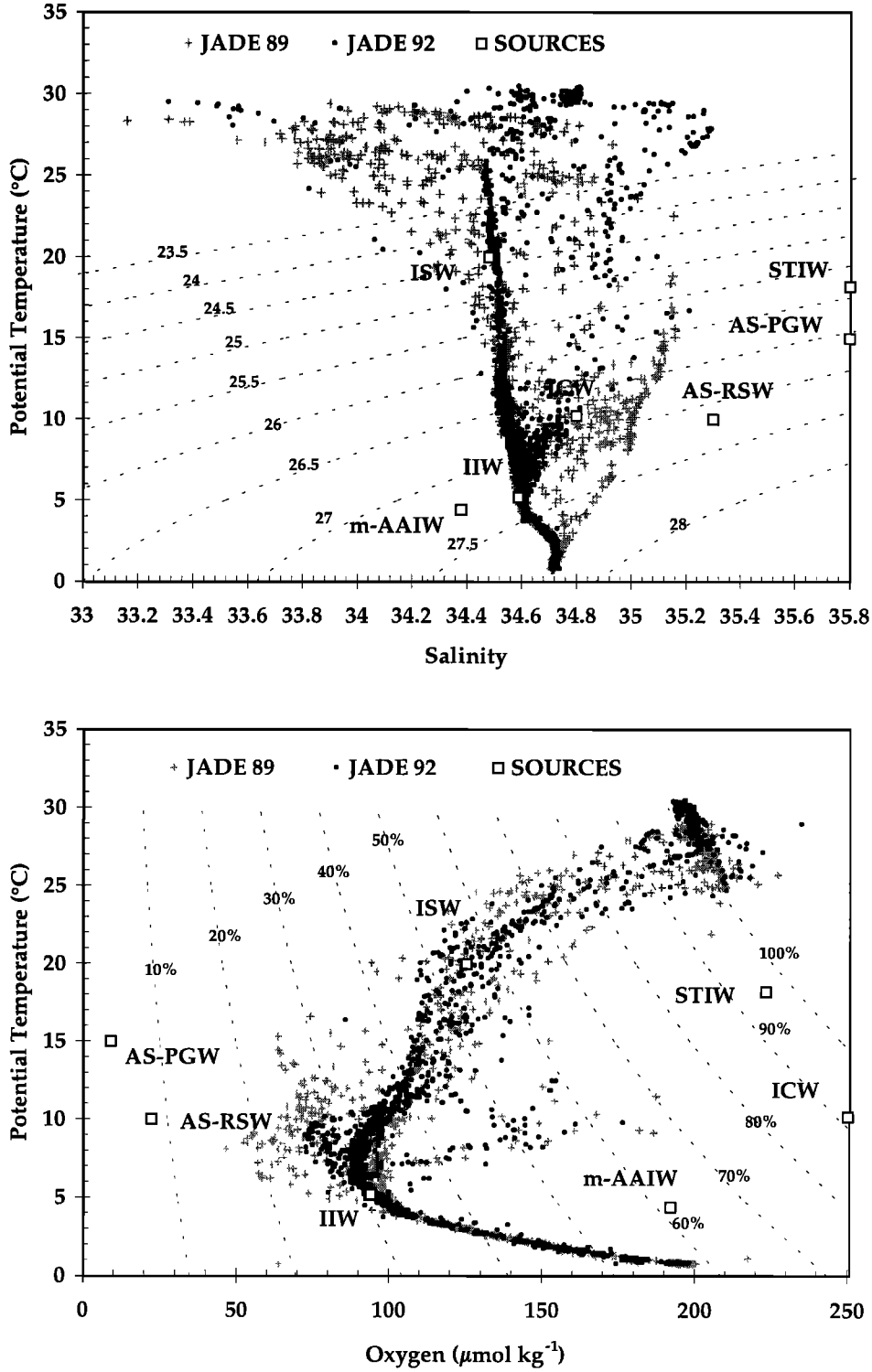

Figure 4. The (top) θ-*S* and (bottom) θ-O_2 diagrams for all stations of JADE 89 and JADE 92 (bottle data). Squares correspond to the location of the sources. Stippled lines indicate the limit study corresponding to the 200-800 m layer. Abbreviations are defined as follows: ISW, Indonesian Subsurface Water; STIW, Subtropical Indian Water; ICW, Indian Central Water; m-AAIW, modified Antarctic Indonesian Water; IIW, Indonesian Intermediate Water; AS-RSW, Arabian Sea-Red Sea Water; and AS-PGW, Arabian Sea-Persian Gulf Water.

output of the Gulf of Aden for the AS-PGW and AS-RSW, respectively.

4.3. Uncertainties

To discuss seasonal variation of mixing coefficients, we first need to examine the possible errors on these coefficients. Thirty perturbations have been realized at each station. A relative error is associated with each tracer according to measurements and source values (Table 2) and is taken into account for each perturbation. These errors represent, for each sample, the variability due to the measurement uncertainties and the temporal (interannual scale) and spatial variations for the defined sources.

Table 2. Tracer Water Source Characteristic and Relative Errors

	STIW	ICW	m-AAIW	ISW	IIW	AS-PGW	AS-RSW	Characterization Error	Measured Value Error
θ, °C	18.2	10.2	4 4	20	5.2	15	10	0.05	0.001
Salinity	35.80	34.80	34.38	34.48	34.59	35.80	35.3	0.005	0.001
O_2, μmol kg^{-1}	223.3	250.1	196.04	125 0	93.79	9	22.33	0.05	0.02
PO_4, μmol kg^{-1}	0.2	0.8	2.0	0.8	2.6	2.4	2.6	0.1	0.05
NO_3, μmol kg^{-1}	2	8	20	10	32	20	30	0.1	0.05
$Si(OH)_4$, μmol kg^{-1}	8	8	22	10	85	30	50	0.1	0.05
σ_θ[a]	25.83	26.76	27.25	24.37	27.33	26.59	27.18		

Abbreviations are defined as follows: STIW, Subtropical Indian Water; ICW, Indian Central Water; m-AAIW, modified-Antarctic Intermediate Water; ISW, Indonesian Subsurface Water; IIW, Indonesian Intermediate Water; AS-PGW, Arabian Sea-Persian Gulf Water; and AS-RSW, Arabian Sea-Red Sea Water.

[a] The density has been calculated from the equation of state of seawater with tracer values defined in this table. (reference pressure= 0dbar)

The standard deviation, computed from the multiparametric analysis and associated with each mixing coefficient, expresses the variation of the water mass from the steady state, which is considered to characterize the sources. High standard deviations are mainly observed in the zone where the defined source waters do not mix. Weak standard deviations are observed at depths where the sources are the best represented.

During the SE monsoon, on the Australia-Bali section and from 200 to 800 m, the uncertainty of the coefficients is 6.2%, 0.1%, 2.2%, 0.4%, 0.8% and 9% for STIW, ICW, m-AAIW, ISW, IIW, and AS-RSW, respectively (AS-PGW is not presented in this section). For the NW monsoon, the uncertainty is 4.5%, 1.5%, 2%, 0.5%, 0.8% and 2%, respectively. These values have been calculated at the locations where the sources have the highest coefficients on the section. They give the confidence limit of the mixing coefficients and allow us to determine if the seasonal variability is meaningful.

4.4. Residuals

The residual vector on the tracers (see (8)) shows high absolute values for some layers of the water column (Figure 6), particularly in the surface layer, which is not taken into account here. When residuals are positive, tracer value is overestimated, and, inversely, negative residuals correspond to an underestimation. The significant residuals in surface layer are explained by the local nonconservation of these tracers. The biological activity, intense in the euphotic zone, acts like a precursor of the nutrient sink and dissolved oxygen source. Potential temperature and salinity residuals show that for a heat gain there is a mass loss (positive salinity surface residuals versus negative potential temperature surface residuals). Between 200 and 800 m and for both seasons, the residuals are low, indicating that defined sources are well adapted for this layer. Consequently, the analysis of the results will be discussed only for the 200-800 m layer.

5. Results of the Inversion: Seasonal Comparison

The results of the inversion with seven sources, three tracers (potential temperature, salinity, and dissolved oxygen), and continuity (mass conservation), are presented in the Figures 7, 8, 9, and 10. They show the proportions of each source along the Australia-Bali section and in the Indonesian Straits.

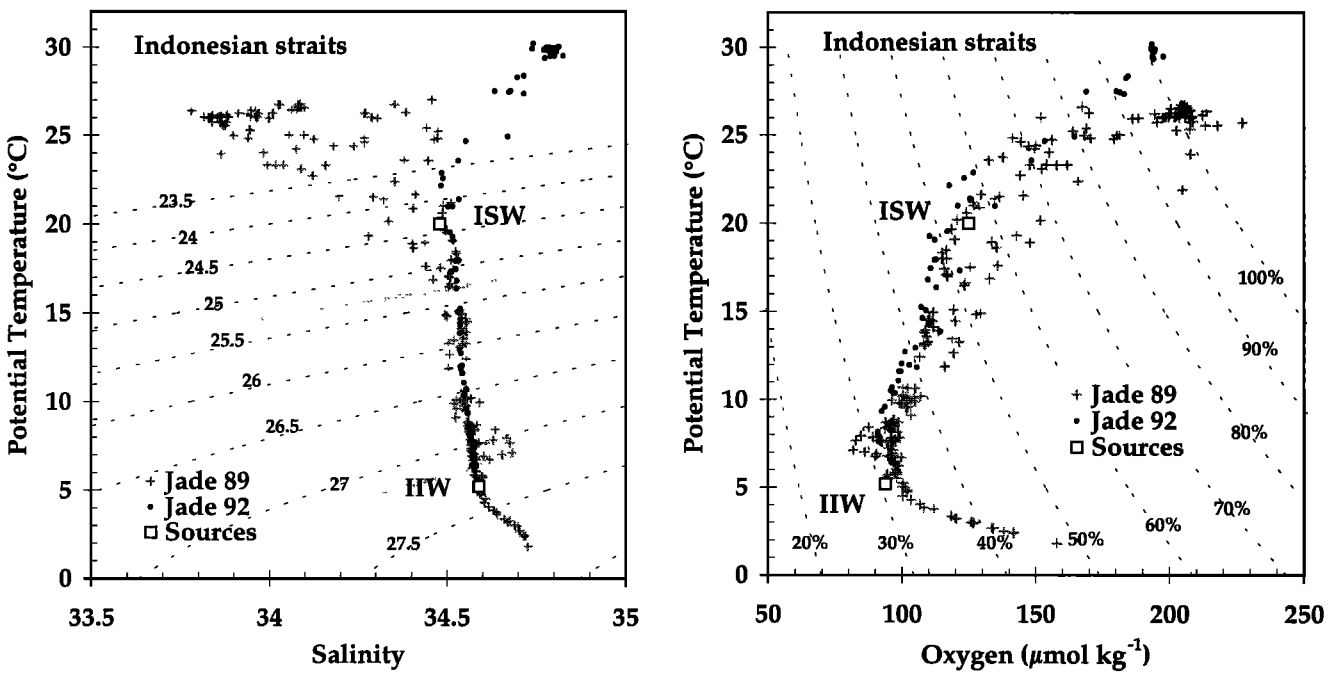

Figure 5. The (left) θ-*S* and (right) θ-O_2 diagrams for stations in the Indonesian Straits (bottle data). Squares correspond to the location of the sources. Stippled lines indicate the limit study corresponding to the 200-800 m layer.

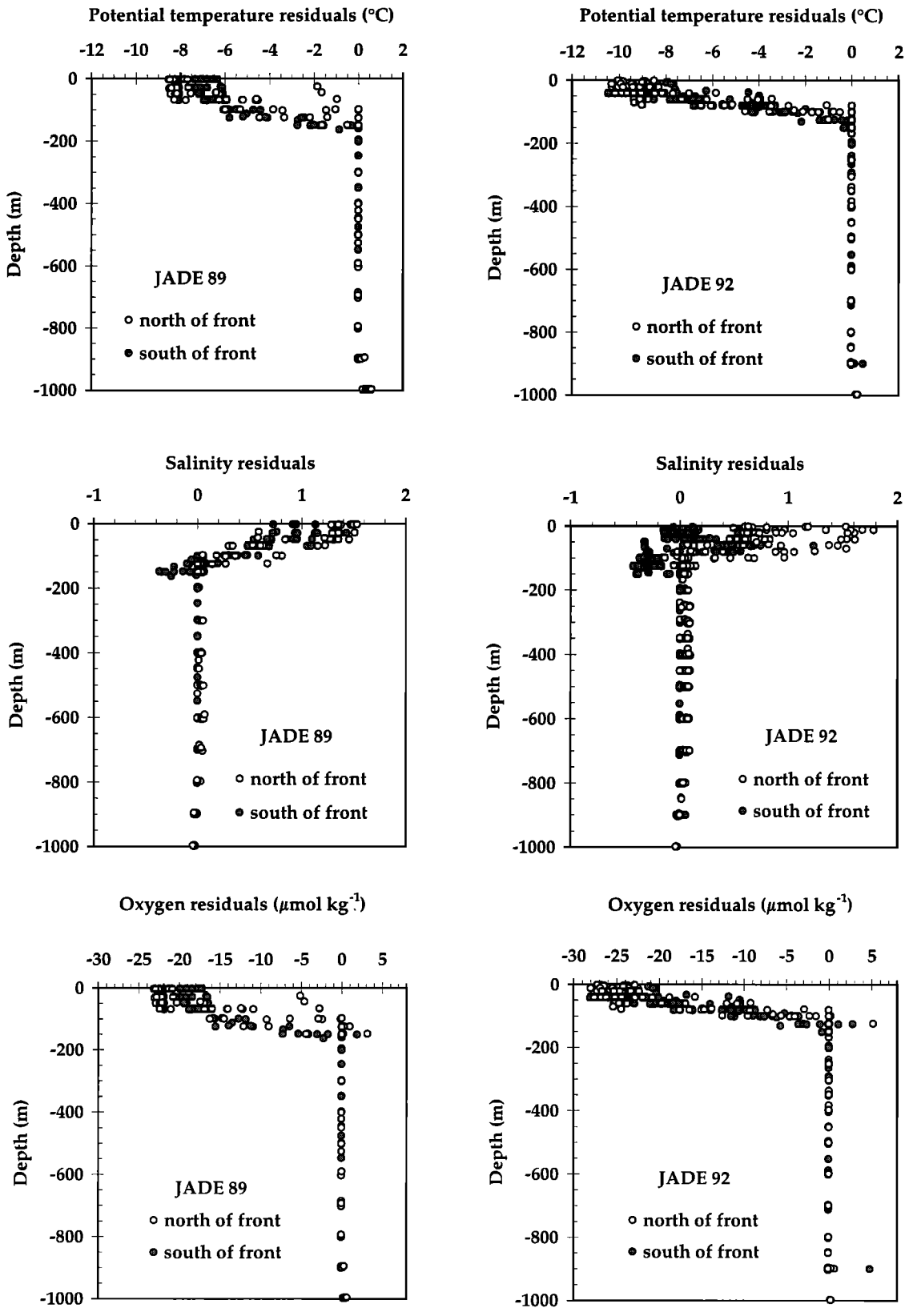

Figure 6. Residuals of (top) heat (°C), (middle) salinity and (bottom) oxygen (μmol kg^{-1}) for (left) JADE 89 and (right) JADE 92 in the Australia-Bali section.

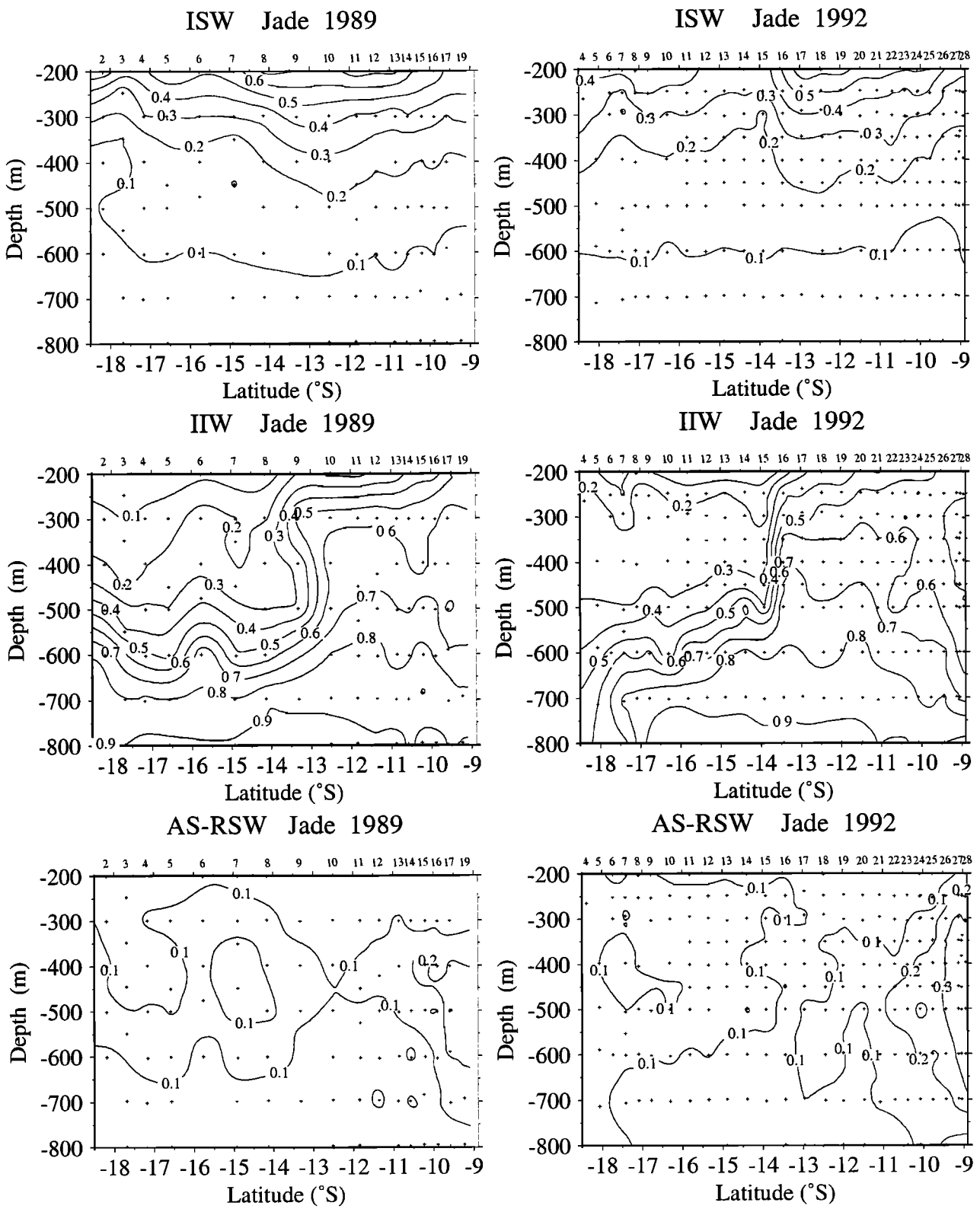

Figure 7. Mixing coefficients of the Indonesian and North Indian water masses in the Australia-Bali section for (left) JADE 89 and (right) JADE 92. Arabian Se-Persian Gulf Water (AS-PGW) is not displayed because it is not present.

5.1. Indonesian Waters

The Indonesian Subsurface Water is present in the thermocline of the Australia-Bali section (Figure 7) with higher values (60%). The ISW is situated between 10°30'S and 14°30'S for the SE monsoon and between 11°30'S and 13°30'S for the NW monsoon. A decrease in the coefficient is observed at the latitude of the hydrological front only for the NW monsoon and at the surface; an accumulation of low-salinity water is observed north of 13°30'S (Figures 3c and 3d). *Godfrey and Ridgway* [1985]

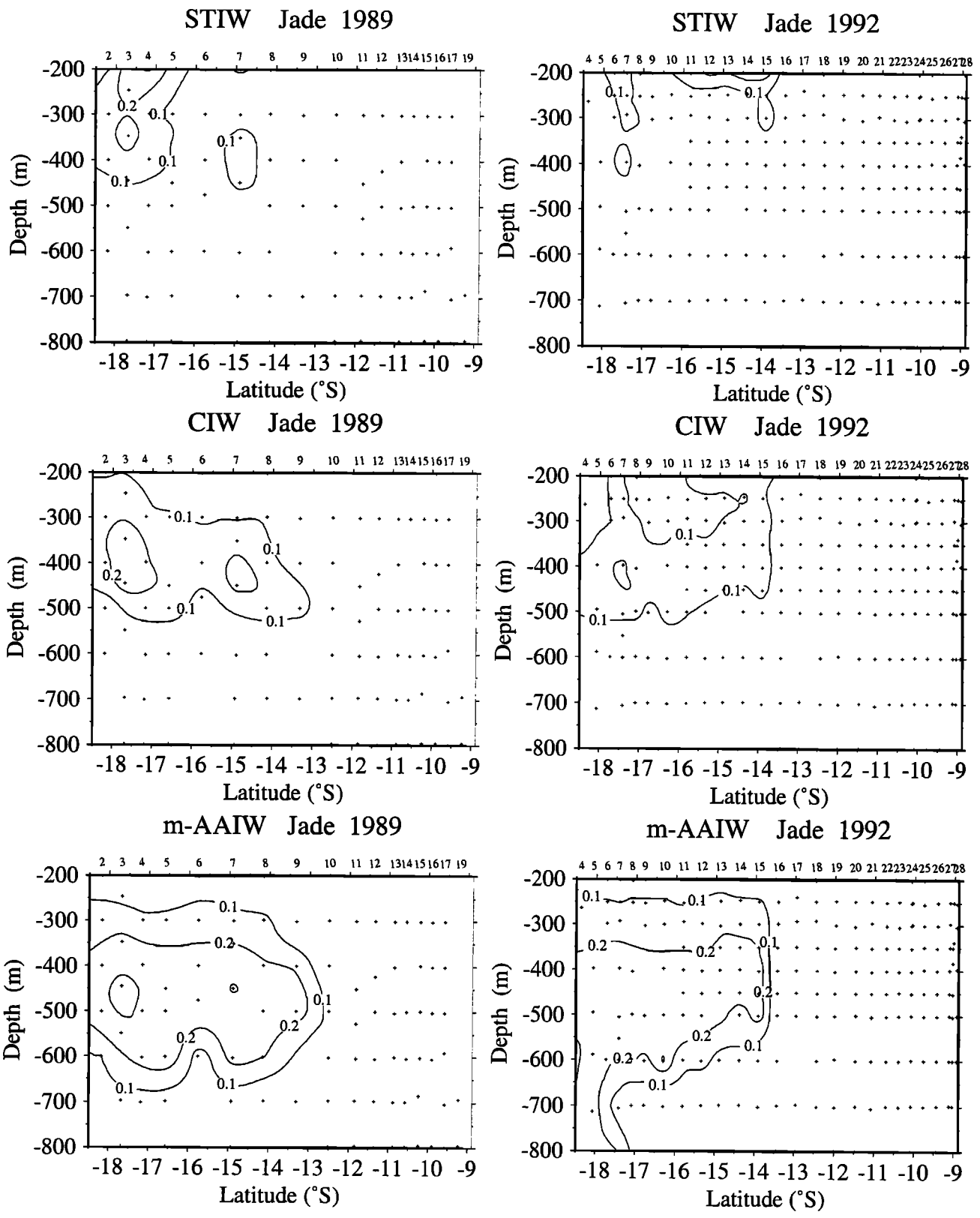

Figure 8. Mixing coefficients of the South Indian water masses in the Australia-Bali section for (left) JADE 89 and (right) JADE 92.

show that part of the South Equatorial Current transports Indonesian waters westward, on the latitude close to 10°S [*Fine*, 1985], and that a fraction of the Indonesian Water flows southward along the West Australian coast in the Leeuwin Current. During the SE monsoon near the Bali coast, an uplift of the mixing coefficient lines corresponds to the presence of upwelling during this season. The salinity distribution, north of the Australia-Bali section [*Fieux et al.*, 1994, Figure 3c, 1996b,

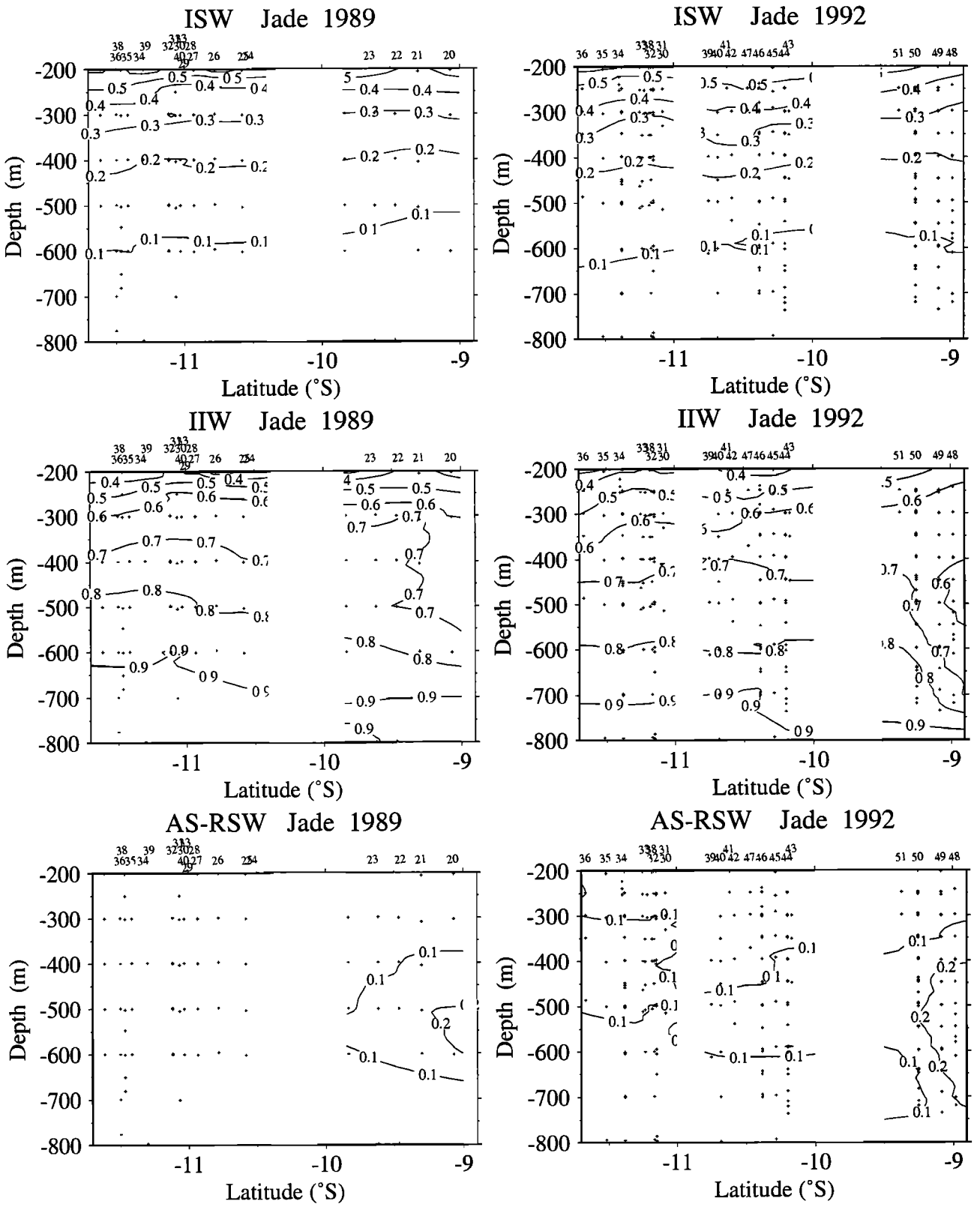

Figure 9. Mixing coefficients of the Indonesian and North Indian water masses in the section of the Indonesian Straits for (left) JADE 89 and (right) JADE 92.

Figure 3c], is in agreement with the decrease of the proportions of the IIW near the Bali coast, which is replaced by the water coming from the North Indian Ocean.

Between Australia and Bali, around 300-350 m, the IIW gradually replaces the ISW. High values (> 55% for both seasons) are observed below 300 m in the northern part of the section (Figure 7). The gradient of isolines showing the hydrological front is stronger during the NW monsoon than during the SE monsoon, possibly owing to closer stations for the NW monsoon. South of the front (Figure 7), between 200 and

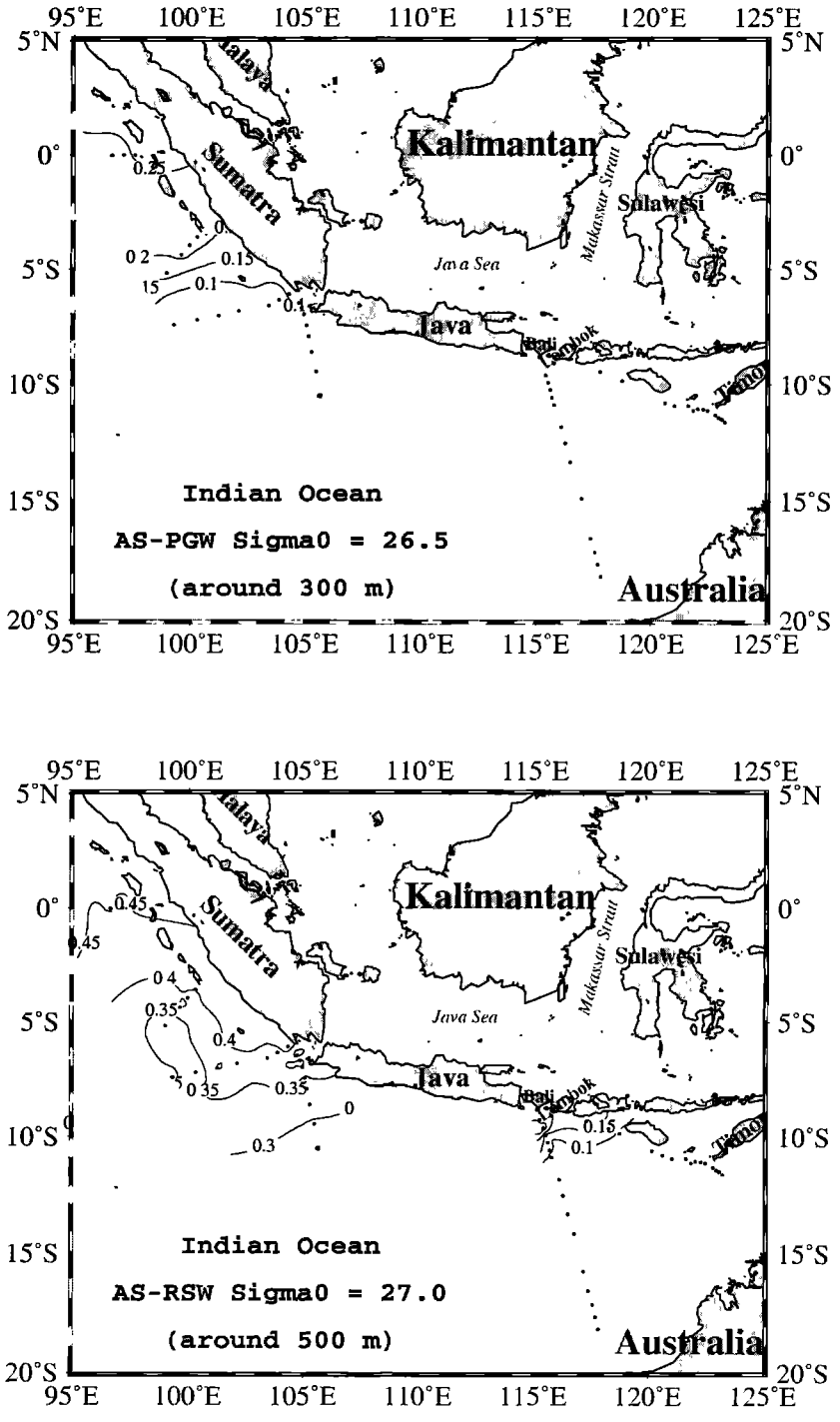

Figure 10. Isopycnal distribution of the mixing coefficients of the north Indian water masses for JADE 89 at (top) 300 m and (bottom) 500 m.

600 m, the IIW appears in slightly higher proportions during the NW monsoon. In 1992 (NW monsoon), the currents are stronger and more irregular than in 1989 (SE monsoon), suggesting an eddy-like circulation, leading to intense mixing between the different waters coming from the southern Indian Ocean and the Indonesian seas [*Fieux et al.*, 1996a]. Below 600 m, the front defined by the mixing coefficients disappears and IIW, at more than 80%, occupies the entire width of the section. Near the Northwest Australian Shelf during the NW monsoon, the proportion values decrease, which is linked to the intrusion of m-AAIW (Figures 7 and 8). Near the Bali coast, a decrease in the IIW mixing coefficient is more prominent during the NW monsoon. This decrease is linked to the increase in the proportion of water coming from the North Indian Ocean.

In and off the Indonesian Straits (Figure 9), the distribution of the ISW is identical for both seasons, without significant seasonal variations of the mixing coefficients. For IIW, few differences are observed between both seasons. At the northern outflow of the Savu Sea, 70% of the IIW is observed at 300 m for the SE monsoon and at 450 m for the NW monsoon on the southern side

(Figure 9). The sections off the Indonesian Straits, during the SE monsoon, were outside the straits. Near the Sumbawa coast, the decrease in the proportion of IIW observed between 400 and 700 m is explained by the introduction of the water originating from the North Indian Ocean, particularly for the NW monsoon when the station measurements were conducted in the strait itself.

5.2. South Indian Waters

Along the Australia-Bali section, the contribution of the three sources (STIW, ICW, m-AAIW) shows small mixing coefficients (<30%) (Figure 8) relative to the selected sources (Table 2). The hydrological front (at 13°30'S) marks the limit of the presence of these Indian waters. Seasonal variations are observed, especially for the Subtropical Indian Water. The STIW is only present between 200 and 300 m in two cores, but the stronger one is at different latitudes, depending on the season. During the SE monsoon, the STIW appears between the latitude 17°S and the Australian coast in weak proportions (10-20%). At the opposite season, the core of the STIW is observed between 14°S and 15°30'S, not deeper than 300 m (<20%). Many physical processes seem to change significantly the characteristics of this source. *Quadfasel et al.* [1996] show that the subtropical flow, north of the NW Cape of Australia, splits in two branches, one part following the shelf break northeastward and the other feeding directly the South Equatorial Current. The first branch could bring the STIW to the northwest of Australia. It is possible that the branches move between the different seasons [*Quadfasel et al.*, 1996]. In the region off the NW Cape, there is a relatively small mean flow with enhanced mesoscale variability [*Quadfasel et al.*, 1996] and, consequently, the STIW is barely represented on the Australia-Bali section. This water as well as the other southern sources (ICW and m-AAIW) are absent in the Indonesian Straits.

The Indian Central Water also shows small mixing coefficients in the Australia-Bali section, appearing inside two cores centered at 400 m (<30%) at 17°30'S latitude and at 450 m (<20%) at 14°30'S latitude for the SE monsoon. As for STIW, the proportion is slightly weaker in the NW monsoon (<20%) (Figure 8). In the southern part of the NW monsoon section, the geostrophic transports show a succession of reversals, which denotes a large mesoscale variability [*Fieux et al.*, 1996a]. This mixing of the Central Indian Water and the Indonesian waters was also observed by *Quadfasel et al.* [1996] in the thermocline off the northwest Australian shelf. In agreement with the IIW distribution in this region, the ICW appears to mix with the IIW when it flows eastward during the NW monsoon. The small proportions observed for the ICW and the STIW suggest that these waters are subject to many changes along their pathways from the anticyclonic subtropical gyre to the northwest of Australia. *Rochford* [1969] showed that the Indonesian waters at 110°E, between 100 and 150 m, characterized by low salinity and mean oxygen content, spread southwards (around 26°S at 110°E) during the NW monsoon (Leeuwin Current). The θ-S diagrams from several sections off NW Australia [*Quadfasel et al.*, 1996] indicate a very strong attenuation of the salinity maximum characterizing the Subtropical Indian Water. Owing to the mesoscale variability observed in 1992 [*Fieux et al.*, 1996a], which could enhance the mixing of the STIW and ICW with IIW, the mixing coefficients for the southern Indian waters are slightly higher in 1989.

The modified Antarctic Intermediate Water is present in a larger proportion than the two other South Indian sources (Figure 8) which is surprising at those depths. It appears inside a core between 350 and 650 m in 1989. In 1992, this water spreads between 300 and 700 m from the Australian coast to the front. *Rochford* [1963] shows the presence of AAIW in the Indonesian Straits but suggests that the hydrological characteristics of AAIW and the Indonesian waters are difficult to separate. *Fine* [1993] shows that some of the recently ventilated AAIW appears to spread both north and northeastward (perhaps to 100°E) into the subtropics and is diluted by water from the Indonesian throughflow. At present, the separation between AAIW and IIW in this strongly mixed region is not well known. The results of this application show no signal of m-AAIW in the Indonesian Straits.

5.3. North Indian Ocean Waters

Two sources flow from the Arabian Sea: the Persian Gulf-Arabian Sea Water (at the isopycnal surface of the salinity maximum of the Persian Gulf water) and the Arabian Sea-Red Sea Water. The only source observed in the Australia-Bali section is AS-RSW (Figure 10), mainly found in the northern part of the section and defined also as North Indian Intermediate Water (NIIW). Its core is centered around 400-600 m (>20%) during the SE monsoon and between 250 and 700 m during the NW monsoon, with a slightly higher coefficient (>30%) in the core (Figure 7). *Fieux et al.* [1996a] show that the intermediate eastward current along the Indonesian coast is stronger in February 1992 than in August 1989. However, this could be the result of better sampling near the coast for the SE monsoon. Nevertheless, the most important contribution of this North Indian Intermediate Water is observed during the NW monsoon and is corroborated by the higher proportions during the northern monsoon in the Indonesian Straits (Figure 9). Mixed AS-PGW and AS-RSW is observed along the Sumatra and Java coasts before reaching the Indonesian archipelago (Figure 10). These waters are flowing from the Arabian Sea to east of the Indian Ocean. The AS-PGW is characterized by high salinity and oxygen maxima spreading between 200 and 300 m. The modified Red Sea water is also characterized by a salinity maximum but at a higher density ($27.2 < \sigma_\theta < 27.4$) than the AS-PGW. This study clearly shows that the water in the Australia-Bali section originates from the mixing of Red Sea Water and Arabian Sea Water, with many modifications occurring along its path and particularly between Sumatra and Bali through mixing with Indonesian seas waters (Figure 10).

6. Biological Tracer Utilization: Comparison for JADE 1989

The seasonal analysis was performed using three tracers and continuity. Seven sources were defined to explain the water mass mix in the eastern Indian Ocean. In order to specify the contribution of the different water masses to the water mass mix, we introduce biological tracers into the multiparametric program. In the eastern Indian Ocean, there are young and old water masses, showing different biological characteristics. Therefore the nutrients become good tracers of these water masses. However, because of their nonconservative behavior, the biological variation of these tracers must be taken into account by introducing a biological unknown (see (2)). This unknown collects together the biological variability in the water mass throughout its route in the oceanic circulation and the variability in the water column of the JADE stations. It allows the study of

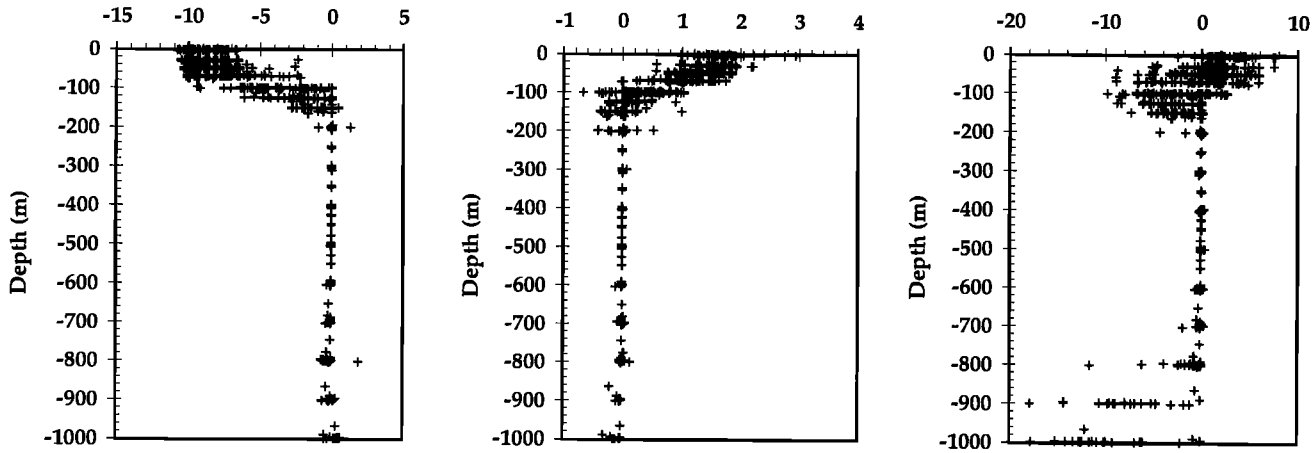

Figure 11. Residuals of (left) heat (°C), (middle) salinity, and (right) silicates (μmol kg^{-1}) for all sections of JADE 89.

the ratios between the biological unknowns and analysis of their evolution in comparison with Redfield ratios. For the seasonal study, the unknown of oxygen was not used, because with only three tracers, the introduction of this parameter would have been equivalent to a small weight on oxygen. Since there were no nutrient data during JADE 92, the application with the nutrient tracers was only possible with the JADE 89 data. A comparison with the results obtained with the *T*, *S*, and O_2 tracers and continuity will be discussed to show the importance of the introduction of nutrients as tracers of water masses.

6.1. Uncertainties, Residuals, and Biological Unknowns

An analysis of the standard deviations shows that the coefficients must be taken with the following accuracy: during the SE monsoon, in the Australia-Bali section, the uncertainty of the coefficients is 0.2%, 4.2%, 3.8%, 0.5%, 0.5%, and 5.8% for STIW, ICW, m-AAIIW, ISW, IIW, and AS-RSW, respectively. For the equator-Sumatra-Java sections, the uncertainties are 0.8%, 0.85%, 2%, and 4.8% for m-AAIIW, IIW, AS-PGW, and AS-RSW, respectively. These values have been calculated at locations where the sources penetrate the section with the highest coefficients.

The residuals for potential temperature, salinity, and dissolved silicate are close to zero for the 200-800 m layer (Figure 11). No residuals are observed for oxygen and nutrient tracers (phosphate and nitrate), because all the variations are given by the biological unknowns (Figure 12). The relation between the biological unknowns $\Delta O_2/\Delta PO_4$ shows a slope (around -178), which is closer to the ratio -175 defined by *Takahashi et al.* [1985] than to the Redfield ratio -138/1 [*Redfield,* 1958]. An the relation between nitrate and oxygen, the slope $\Delta O_2/\Delta NO_3$ (≈ -7) is slightly lower than the Redfield ratio (-138/16 ≈ -8.625) [*Redfield,* 1958]. The analysis of the data set shows that the few remote points, with a low value of ΔNO_3 and a high value of ΔO_2 (Figure 12), correspond to the section near the equator and Sumatra. The low values of ΔNO_3 are observed in the water masses coming from the Arabian Sea. The water masses formed in the North Indian Ocean are subject to intense biological

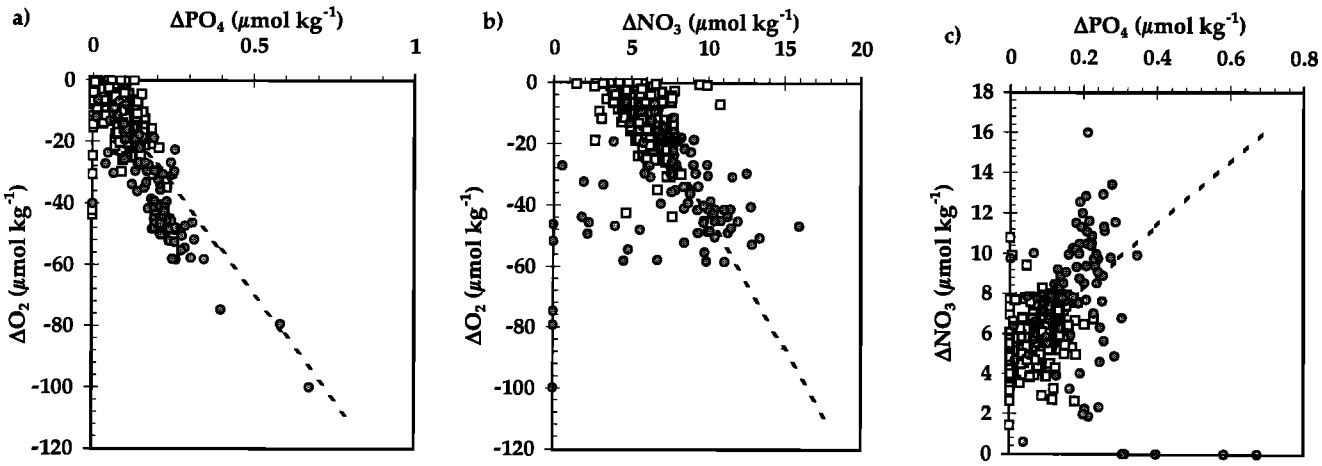

Figure 12. Relation between the parameters of biological variation for all sections of JADE 89. Squares represent the Bali-Australia Straits sections, and circles represent the equator-Sumatra-Java sections. Comparisons with the Redfield ratio (dashed line) are $-O_2/P$, -138/1; $-O_2/N$, -138/16; and N/P, 16/1. (a) ΔO_2=-178.40ΔPO_4 - 2.40 (number of samples *n*=310, correlation coefficient *r*=0,834); (b) ΔO_2=-6.92ΔNO_3 + 34.05 (*n*=303, *r*=0.334); and (c) ΔNO_3=25,76ΔPO_4 (*n*=308, *r*=0.221).

activity. Large oxygen depletion is seen in the Arabian Sea at 200 m [*Mc Gill*, 1973]. In this zone of the Arabian Sea, denitrification and nitrogen fixation modify the nitrogen pool, and therefore the ratios between the biological elements are different from the Redfield ratios generally observed in the ocean. Low N/P ratios are expected in regions of strong denitrification in the water column. If we do not take into account these distant points, the distribution of the points shows a slope close to the N/P Redfield ratio. The ratio $\Delta NO_3/\Delta PO_4$ ($\approx$ 26) observed from the JADE data (Figure 12) is higher than the ratio 16/1 defined by *Redfield* [1958] because of the high values of ΔNO_3 that deviate from the general distribution. These high values are also found on the equator section. The distribution of these unknowns in the Bali-Australia section and Indonesian Straits (Plate 1) is in agreement with biological processes in the water masses. Small ΔO_2 values are observed south of the front, where the Southern Indian Water is located. Large ΔO_2 values are observed north of the front, where waters coming from the Indonesian seas and the North Indian Ocean are present. Although the biological unknowns should contain information on both local and remote export production through remineralization processes within the water masses, their spatial distribution also reflects part of the long-term (annual and large scale) primary production in the investigated area. Such analysis is presented in Figure 13, where the results of ΔO_2, ΔNO_3, and ΔPO_4 have been averaged over the depth range 200-800 m. These results are compared to the large-scale primary production fields calculated by *Antoine et al.* [1996] using the coastal zone color scanner (CZCS) climatology of chl *a*. The distribution of annual primary production derived from remote sensing observation and extracted along the JADE track (Australia-Bali, Figure 13) presents large values in the north of the section, a "plateau" in the frontal area (12°S–14°S), and a minimum at around 17°S. Near the coast of Australia, we also note a slight increase in primary production. The biological unknowns for oxygen and nutrients do not follow perfectly this distribution. However, there is a trend of high values in the north and low values in the south of the section (note the inverse axes for oxygen), indicating that the biological unknowns captured regional memory of biological activity. Differences between the two fields, such as the high values in ΔPO_4 at 13°S, may be related to the "instantaneous" picture obtained with the JADE 89 data compared to average estimation of primary production calculated with composite fields of 8 years of satellite imagery including the interpolation procedure. In addition, the biological unknowns are associated not only to local information in export production (vertical sedimentation) but also to advective transport (horizontal) of remineralized material produced in remote surface layers. For example, the high variability in the north and peaks in ΔO_2 and ΔPO_4 observed at 13°S are certainly related to significant input of material from Indonesian waters, a signal coherent with geostrophic transport. In more detail, it is interesting to find a high ΔPO_4 signal around 300 m between stations 9 and 10 (Plate 1 and Figure 13), at the same pair of stations where a westward subsurface current of 20 cm s^{-1} around 200 m has been calculated [*Fieux et al.*, 1996a]. On the other hand, the reason why this signal is apparent in ΔPO_4 and ΔO_2 distribution but not in ΔNO_3 remains an open question.

In the Indonesian Straits (Plate 1), nutrient and oxygen unknowns are large at depths of 350-400 m. The characteristics of the sources from the Indonesian seas and the South Indian Ocean are different from those of the North Indian Ocean. On the section, the sources originating from the South Indian Ocean are younger water masses (see CFC distribution of *Fieux et al.* [1996b]) and, consequently, poor in nutrients and rich in oxygen. The biological activity in those water masses is less important. The water masses coming from the Indonesian seas are rich in dissolved silicate, and those coming from the North Indian Ocean have undergone intense biological activity. This variability in the biological characteristics allows us to better separate the sources and, consequently, give supplementary information about the water masses.

6.2. Water Masses

The distribution of the water masses is presented in Figures 14, 15, 16, 17, and 18. Some quantitative differences are shown in comparison with the analysis using the *T*, *S*, and O_2 tracers. These differences are observed for the Indian waters, especially for the North Indian Ocean sources and the modified Antarctic Intermediate Water.

6.2.1. Indonesian waters. The Indonesian waters show the same spatial distribution (Figures 14 and 15), with slightly lower mixing coefficients for the IIW (<60% above 500 m, north of 13°30'S) in agreement with *Rochford* [1963]. In the Indonesian Straits (Figures 9 and 15), the contribution of IIW is less marked for depths shallower than 500 m.

6.2.2. South Indian waters. The STIW is represented by a low mixing coefficient (Figures 8 and 14). In comparison with the results obtained with the three tracers, there is a slight difference in its distribution inside one core (Figure 8). The ICW is present inside two cores (>20%) centered around 400 m at 17°30'S and 450 m at 14°50'S (Figure 13), at the same latitudes and depths pointed out in the analysis without nutrients (Figure 8) but with slightly higher coefficients for the core at 17°30'S. Two cores appear in the m-AAIW distribution. They are centered around 450-500 m, similar to the distribution obtained from the hydrological multiparametric analysis. The m-AAIW appears slightly below the ICW. These depths (450-500 m) correspond to σ_θ=26.8-27.0. *Rochford* [1963], using a salinity frequency analysis, shows that the AAIW spreads between Bali and Australia at σ_θ=27.00. He also shows, at σ_θ=26.90, the presence of the AAIW along both sides of Timor and at σ_θ=27.00, west of Timor. In the Indonesian Straits section (Figure 15), the m-AAIW is also found west of Timor but between 250 and 500 m and mainly centered at 300 m around σ_θ=26.60, which is quite different. There is no indication of a connection between the Timor Sea and the west Australian coast. *Rochford* [1963] suggests that, at temperatures and salinities higher than the minimum salinity, the characteristics of the AAIW merge into the characteristics of the Indonesian waters. Both the Antarctic and Indonesian Intermediate Waters are identified by a salinity minimum, and their identification becomes very difficult with only hydrological tracers. In the same way, the hydrological and biological characteristics of the ISW (Table 2) can become close to those of m-AAIW at intermediate depths. Consequently, it is possible that the presence of m-AAIW in the Indonesian Straits results from an incomplete separation between m-AAIW and ISW. An earlier study [*Fine*, 1993] suggests that the AAIW appears to spread both north and northeastward into the subtropics. There, the properties of recently ventilated AAIW appear to be diluted by water from the Indonesian throughflow. On the sections occupied at the equator and off Sumatra and Java (Figure 16), the AAIW is also found around 400 m (mixing coefficient about 20%). However, *Wyrtki* [1961, 1971] shows a salinity minimum at σ_θ=27.4 (depth around 700 m) near Sumatra as the last trace of the Antarctic Intermediate Water sinking along the Antarctic Polar Front. With the multiparametric analysis on

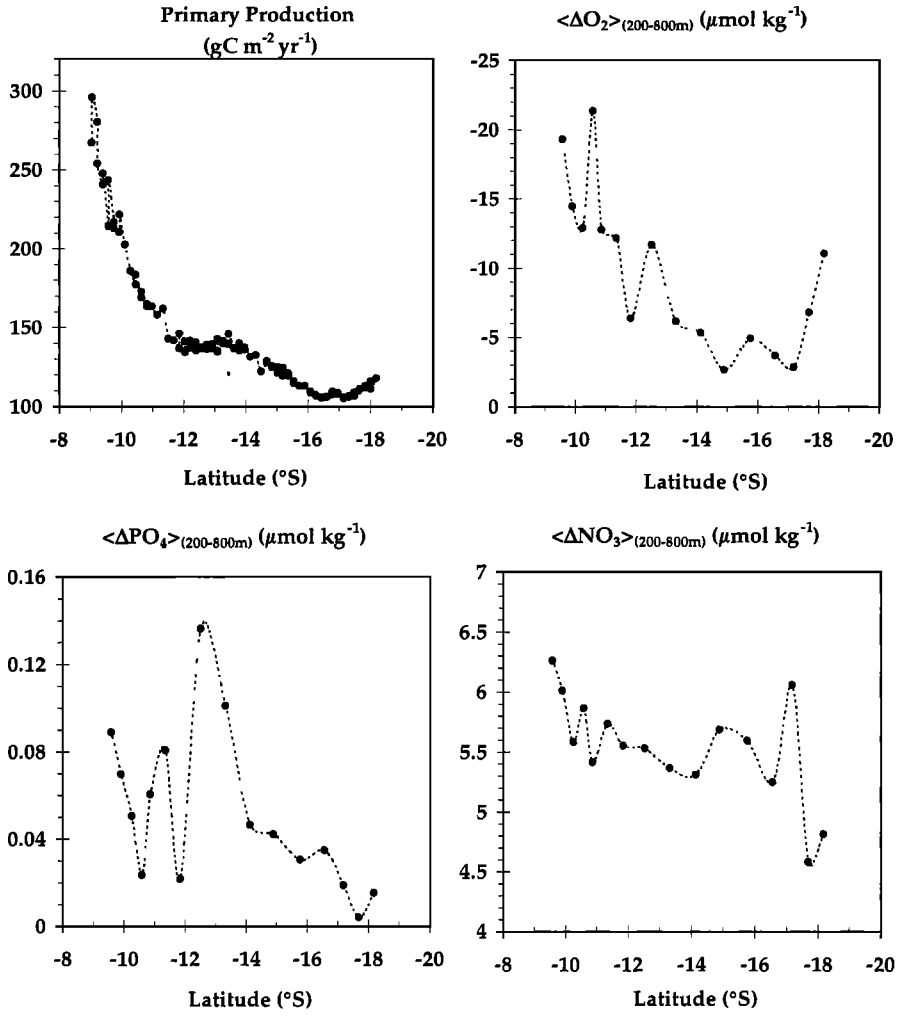

Figure 13. Comparison between primary production (gC m^{-2} yr^{-1}) and the average of the biological unknowns (ΔO_2, ΔPO_4, and ΔNO_3) (μmol kg^{-1}) in the 200-800 m layer for the Australia-Bali section. Values of primary production have been calculated from satellite data.

the three tracers and continuity, m-AAIW and IIW are not meaningfully represented on the sections between the equator and Java.

6.2.3. North Indian Ocean waters. High nutrient concentrations and low oxygen content characterize the North Indian waters. These characteristics are due to important biological activity in the Arabian Sea and from the effects of the upwelling producing living matter requiring oxygen [*Wyrtki*, 1971]. Along the sections from the equator to the straits, we can observe the spreading of these water masses (Figures 17 and 18) during the SE monsoon. The AS-PGW is observed between 200 and 600 m (<25%), and AS-RSW is present below 550 m (>25%) in the Equator section. Along its path to the Australia-Bali section, the proportions of the AS-PGW decrease rapidly and are not observed near Bali (Figure 18). Its composition is significantly modified between the sections situated south of Sumatra and west of Java. These changes in the distribution can come from the influence of the outflow of the Indonesian Sea Water (Figure 16), which can be followed along Java and Sumatra from the high silicate values. This difference is relatively small in the AS-RSW distribution. It shows a spreading close to the Indonesian coasts below 400 m (>20%). A core of the AS-RSW (>35%) is also observed around 700-800 m at the equator. The analysis of the mixing coefficients shows that AS-RSW coefficients are high below 800 m along Sumatra. However, all residual values increase below this depth, suggesting that these coefficients may not be meaningful. Nevertheless, this observation is corroborated by the definition of the core layer of RSW by *Wyrtki* [1971]. Consequently, the introduction of the nutrients into the multiparametric system further constrains the system. The results are in good agreement with data published earlier [*Wyrtki*, 1971; *Fieux et al.*, 1994, 1996a, b].

7. Conclusions

In this paper, we have presented a new way of looking at the JADE data. The results of the multiparametric analysis, between 200 and 800 m, are in good agreement with the present knowledge of the water mass circulation in the Indonesian throughflow. Using two seasonal hydrographic data sets from the JADE cruises, the estimated proportions of mixing of the water masses show seasonal variations, particularly for the northern and southern Indian Ocean waters. During the SE monsoon, the South Indian Ocean waters (STIW, ICW, and m-AAIW) appear south of the hydrological front by intrusion from the northwest Australia region, with proportions slightly increasing with depth.

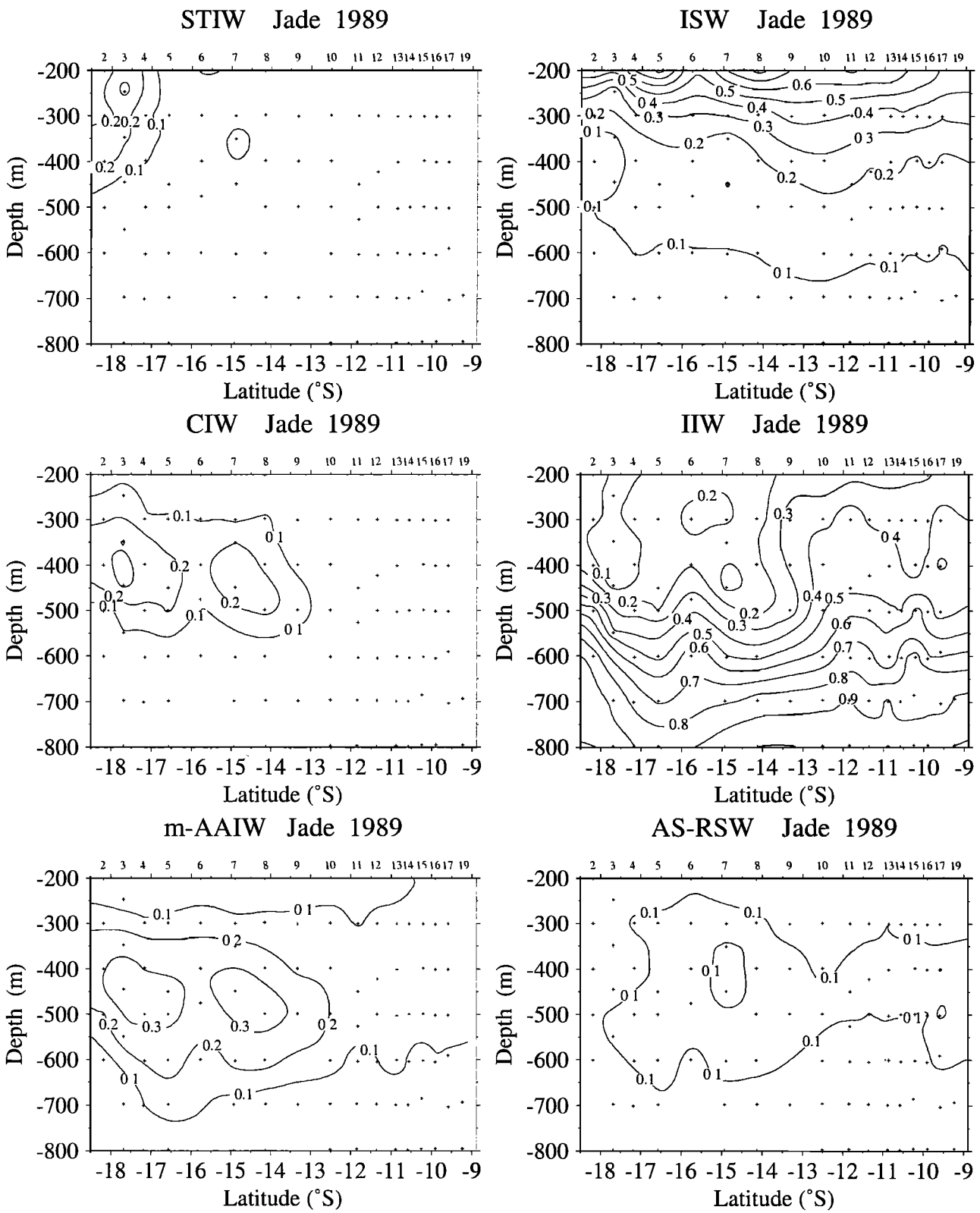

Figure 14. Mixing coefficients of the Indonesian and South and North Indian water masses in the Australia-Bali section for JADE 89 (with the multiparametric system using nutrients).

Near the Bali coast, only AS-RSW is present with small mixing proportions. The AS-PGW flows from the Arabian Sea along the Sumatra coast and vanishes south of the Sumatra Island. The Indonesian waters have high mixing proportions between 13°30'S and 10°30'S for the subsurface water. The IIW is present below 500 m over the whole section from Bali to Australia. During the NW monsoon, the contribution of the three sources from the South Indian Ocean is relatively less important.

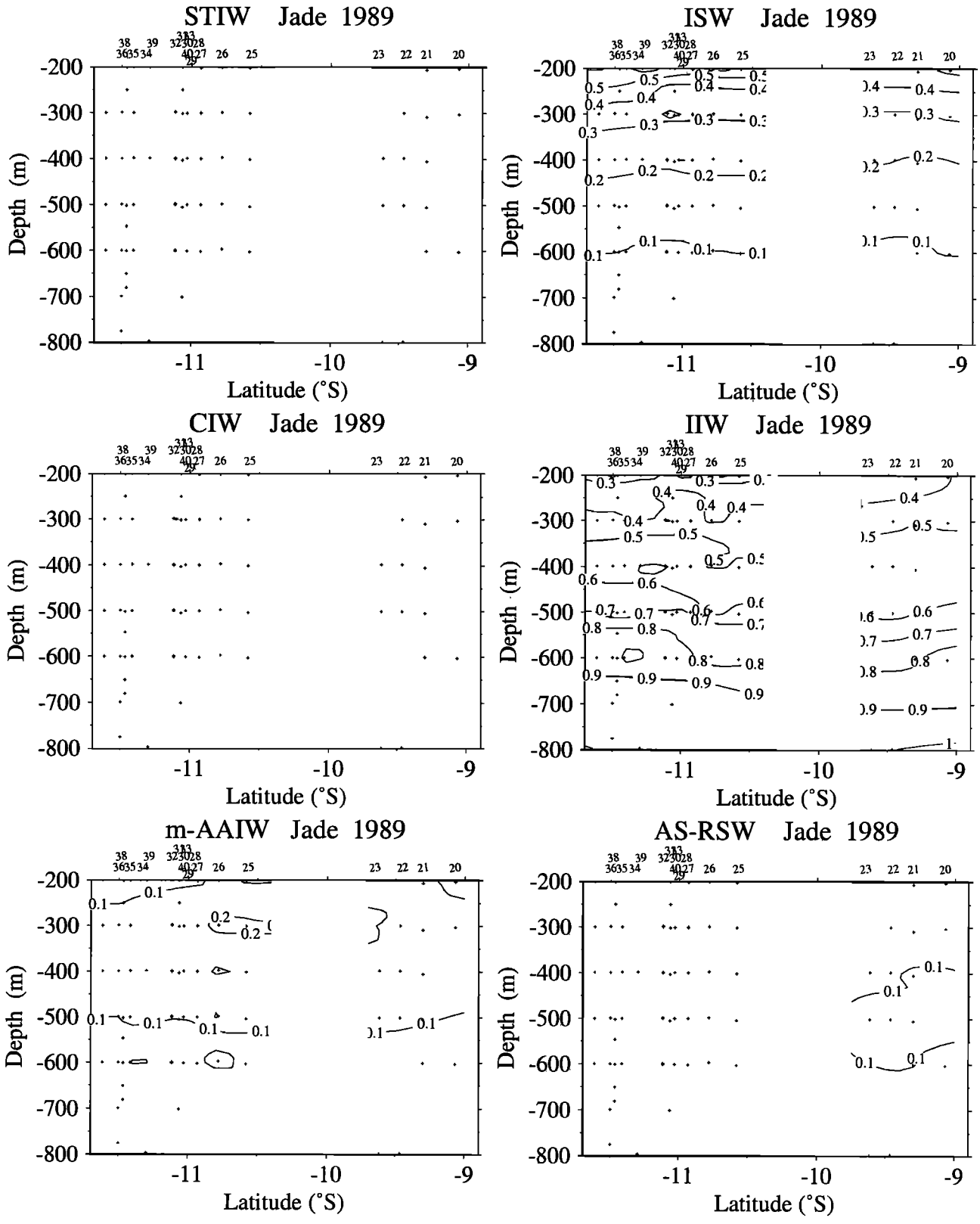

Figure 15. Mixing coefficients of the Indonesian and South and North Indian water masses in the Indonesian Straits section for JADE 89 (with the multiparametric system using nutrients).

Their cores of distribution show variations, particularly for the ICW. These variations are due to strong mesoscale variability in the southern part of the Bali-Australia section, also shown by *Bray et al.* [1997]. During the NW monsoon, the STIW is practically missing below 200 m. Near the Bali coast, the AS-RSW appears with slightly higher mixing proportions and is further observed in the northern Indonesian Strait. The Indonesian waters show similar distributions in the two seasons.

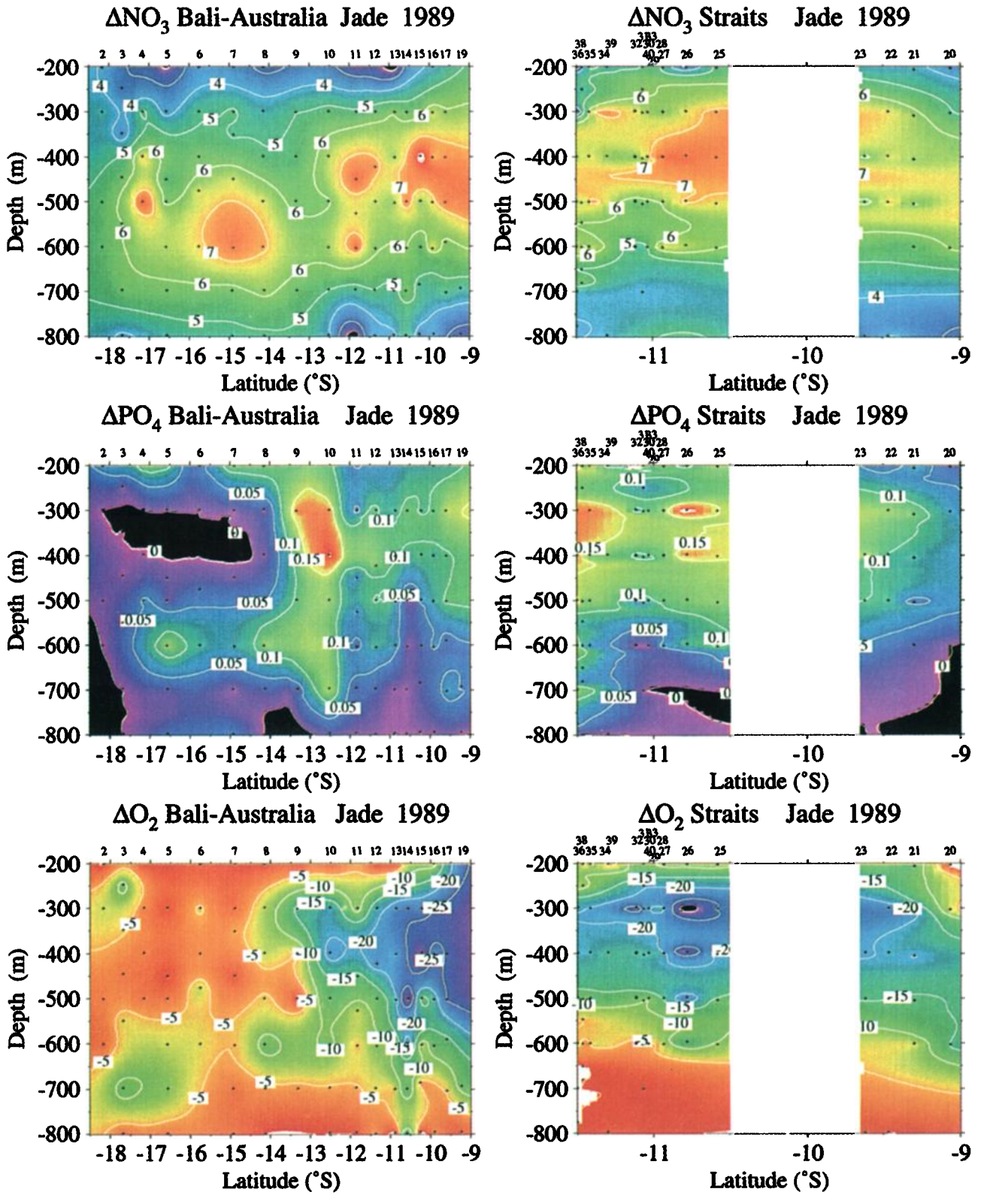

Plate 1. Distribution of the biological variation parameters (ΔO_2, ΔPO_4, and ΔNO_3) in the Australia-Bali section in the Indonesian Straits for JADE 89.

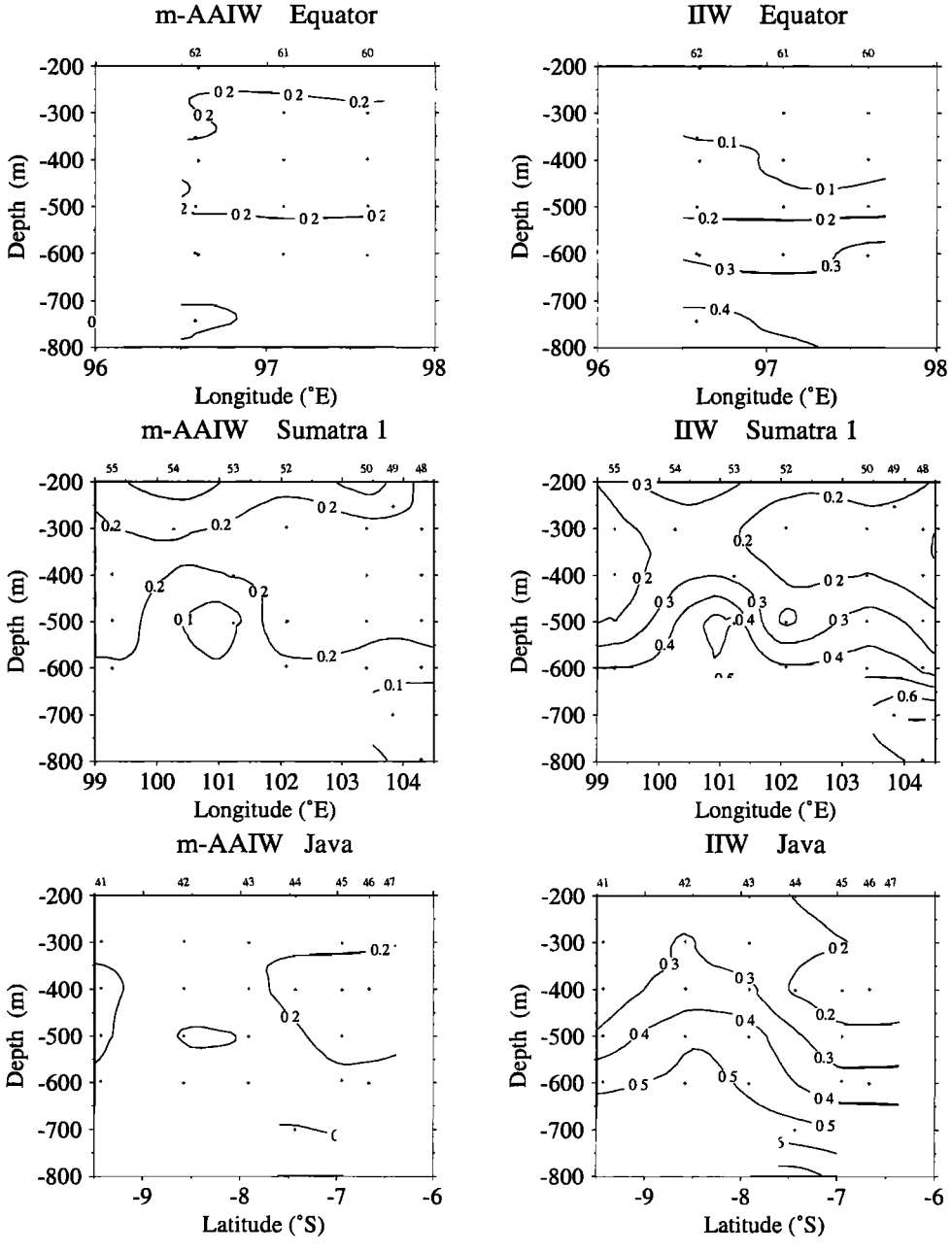

Figure 16. Mixing coefficients of the m-AAIW and IIW in the equator, Sumatra, and Java sections for JADE 89 (with the multiparametric system using nutrients).

The mixing coefficients (in relation to the defined sources) allowed us to show that the Indian Ocean water masses are subject to strong mixing off NW Australia as well as north of the Indian Ocean before reaching the input from the Indonesian archipelago. Moreover, they show that the monsoon system generates seasonal variability of the water mass distribution with, notably, a slightly greater presence of North Indian Ocean waters during the NW monsoon and South Indian Ocean waters during the SE monsoon. Other variations, principally interannual, also play a role in the distribution of the water masses. The JADE cruises were performed in 1989, at the end of a La Niña phase (leading to an increase of rainfall in the region) and in 1992 during an episode of El Niño (decreasing rainfall in the Indo-Pacific region) [*Fieux et al.*, 1996a, b]. These climatic events also act upon the typical magnitude of the throughflow [*Meyers*, 1996]. Therefore the data analyzed for the seasonal study might be subject to the likely interannual effects resulting from the climatic context of the JADE cruises.

The results of the inversion using the nutrients do not show important changes in the general structure of the water mass distribution. Supplementary information in the mixing analysis can be obtained for several water masses such as m-AAIW observed inside the Indonesian Straits. However, as suggested by *Rochford* [1963], the characteristics of m-AAIW and Indonesian waters are very close in the studied region. Consequently, the distribution of m-AAIW at shallow depth can result from an incomplete separation between m-AAIW, ISW, and IIW. The separation between the AS-PGW and AS-RSW distributions is

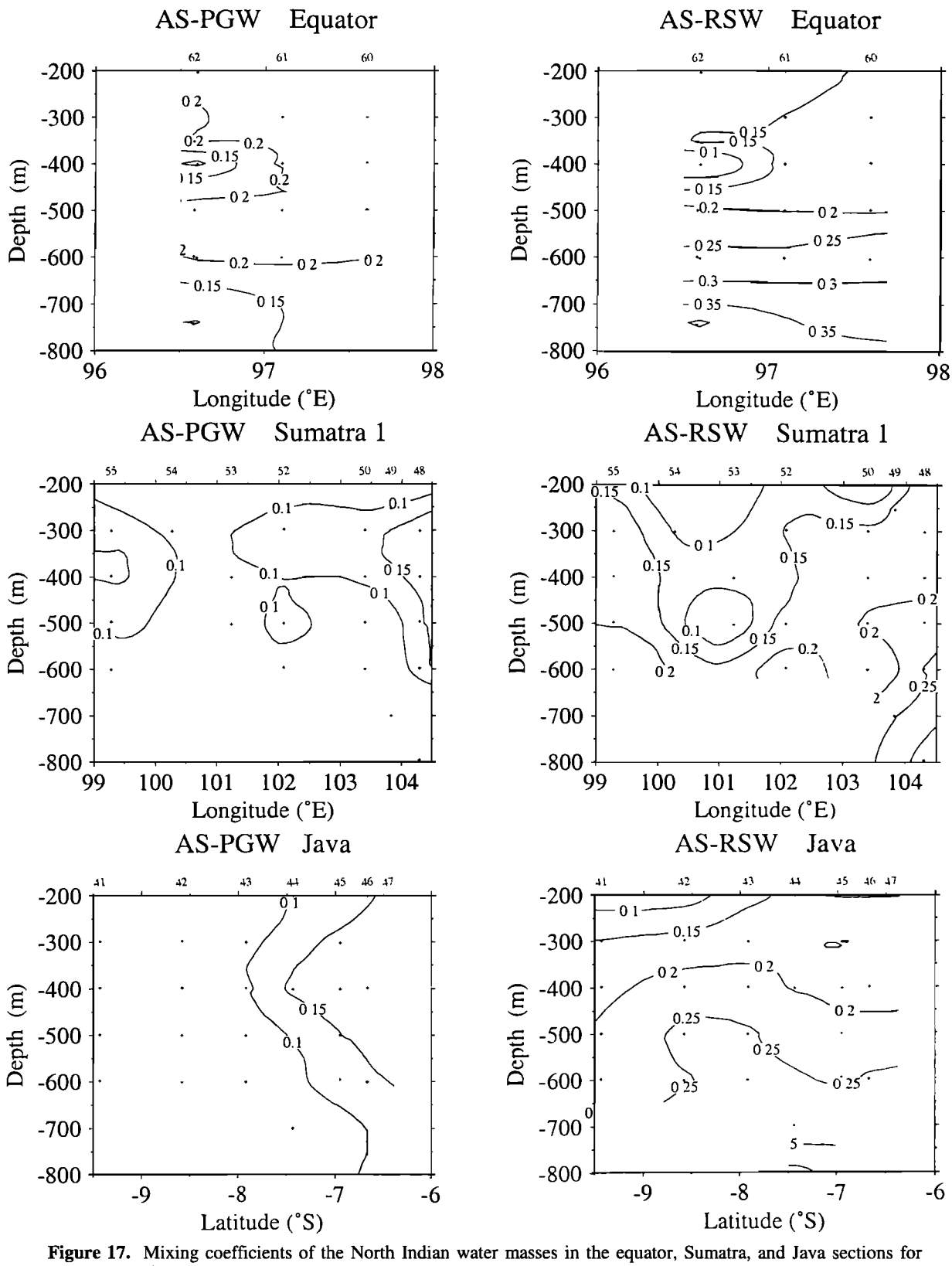

Figure 17. Mixing coefficients of the North Indian water masses in the equator, Sumatra, and Java sections for JADE 89 (with the multiparametric system using nutrients).

well represented along Sumatra and Java. Lower mixing coefficients of AS-RSW can be explained by the presence of IIW along Java and Sumatra constrained by silicate. The AS-RSW is also observed at deeper levels along these islands, in agreement with the definition of this core layer by *Wyrtki* [1971].

This study confirms the usefulness of nutrients as water mass tracers. The introduction of biological parameters makes it possible to separate the variations in nutrients from biological activity on one hand and from dynamics on the other hand. Future analysis will allow the separation of changes in nutrients

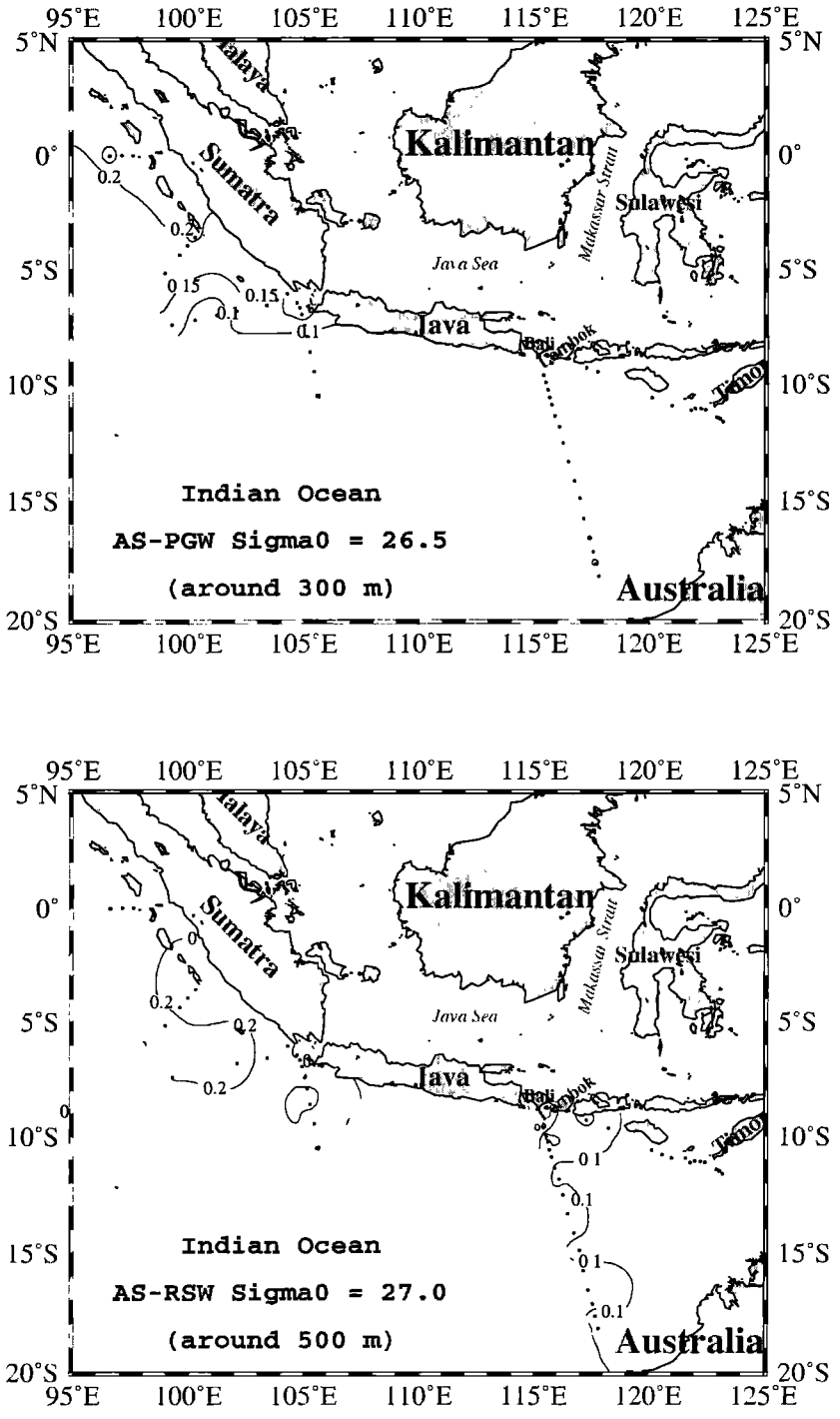

Figure 18. Isopycnal distribution of the mixing coefficients of the North Indian water masses for JADE 89 (with the multiparametric system using nutrients).

from local biological activity as well as biological activity along the path of the water mass. Such analysis will allow greater understanding of the changes in the biogeochemical cycle in response to oceanic circulation.

Acknowledgments. The support of the IFRTP, INSU-CNRS, and the French Embassy in Jakarta, together with the support of the Indonesian BPPT and the Puslitbang Osealonogi LIPI, are greatly acknowledged We thank A.G. Ilahude for his helpful collaboration. We thank all the persons who participated in the collection of the hydrological data and made the measurements of salinity, oxygen, and nutrients during the two cruises.

References

Antoine, D., J. M. André, and A. Morel, Oceanic primary production, 2, Estimation at global scale from satellite (coastal zone color scanner) chlorophyll, *Global Biogeochem Cycles, 10*, 57-69, 1996.

Bolin, B., A. Björkström, K. Holmèn, and B. Moore, The simultaneous use of tracers for oceans circulation studies, *Tellus, Ser. B, 35*, 206-236, 1983.

Bray, N. A., S. Hautala, J Chong, and J. Pariwono, Large-scale sea level, thermocline, and wind variations in the Indonesian throughflow region, *J. Geophys. Res , 101*, 12,239-12,254, 1996.

Bray, N. A., S. E. Wijffels, J. C Chong, M. Fieux, S. Hautala, G.

Meyers, and W. M. L. Morawitz, Characteristics of the Indo-Pacific throughflow in the eastern Indian Ocean, *Geophys Res. Lett., 24,* 2569-2572, 1997

Broecker, W. S., W. C. Patzert, J. R. Toggweiler, and M. Stuiver, Hydrography, chemistry and radioisotopes in the southeast Asian basins, *J. Geophys. Res., 91,* 14,345-14,354, 1986.

Chiswell, S. M., K. A. Donohue, and M. Wimbush, Variability in the central equatorial Pacific, 1985-1989. *J. Geophys. Res., 100,* 15,849-15,863, 1995.

Ffield, A., and A. Gordon, Vertical mixing in the Indonesian thermocline, *J. Phys. Oceanogr., 22,* 184-195, 1992.

Ffield, A., and A. Gordon, Tidal mixing signatures in the Indonesian Seas, *J. Phys. Oceanogr., 26,* 1924-1937, 1996.

Fieux, M., C. Andrié, P. Delecluse, A. G. Ilahude, A. Karvatseff, F. Mantisi, R. Molcard, and J. C. Swallow, Measurements within the Pacific-Indian oceans throughflow region, *Deep Sea Res., Part I, 41,* 1091-1130, 1994.

Fieux, M., R. Molcard, and A. G. Ilahude, Geostrophic transport of the Pacific-Indian Oceans throughflow, *J. Geophys. Res., 101,* 12,421-12,432, 1996a.

Fieux, M., C. Andrié, E. Charriaud, A. G. Ilahude, N. Metzl, R. Molcard, and J. C. Swallow, Hydrological and chlorofluoromethane measurements of the Indonesian throughflow entering the Indian Ocean, *J. Geophys. Res., 101,* 12,433-12,454, 1996b.

Fine, R. A., Direct evidence using tritium data for throughflow from the Pacific into the Indian Ocean, *Nature, 315,* 478-480, 1985.

Fine, R. A., Circulation of Antarctic intermediate Water in the Indian Ocean, *Deep Sea Res., Part I, 40,* 2021-2042, 1993.

Fine, R. A., R. Lukas, F. M. Bingham, M. J. Warner, and R. H. Gammon, The western equatorial Pacific: A water mass crossroads, *J. Geophys. Res., 99,* 25,063-25,080, 1994.

Fu, L., Mass, heat and freshwater fluxes in the South Indian Ocean, *J. Phys. Oceanogr., 16,* 1683-1693, 1986.

Godfrey, J. S., and K. R. Ridgway, The large-scale environment of the poleward-flowing Leeuwin Current, Western Australia: Longshore steric height gradients, wind stresses and geostrophic flow, *J. Phys. Oceanogr., 15,* 481-495, 1985.

Godfrey, J. S., A. C. Hirst, and J. Wilkin, Why does the Indonesian throughflow appear to originate from the North Pacific?, *J. Phys. Oceanogr., 23,* 1057-1086, 1993.

Gordon, A. L., Interocean exchange of thermocline water, *J. Geophys. Res., 91,* 5037-5046, 1986.

Gordon, A. L., and R. A. Fine, Pathways of water between the Pacific and Indian oceans in the Indonesian Seas, *Nature, 379,* 146-149, 1996.

Gordon, A. L., A. Ffield, and A. G. Ilahude, Thermocline of the Flores and Banda Seas, *J. Geophys.Res., 99,* 18,235-18,242, 1994.

Hautala, S. L., J. L. Reid, and N. Bray, The distribution and mixing of Pacific water masses in the Indonesian Seas, *J. Geophys. Res., 101,* 12,375-12,389, 1996.

Hinrichsen, H. -H., and M. Tomczak, Optimum multiparameter analysis of the water mass structure in the western North Atlantic Ocean, *J. Geophys. Res., 98,* 10,155-10,169, 1993.

Kindle, J. C., and P. A. Phoebus, The ocean response to operational westerly wind bursts during the 1991-1992 El Niño, *J. Geophys. Res., 100,* 4893-4920, 1995.

Lawson, C. L., and R. J. Hanson, *Solving Least Square Problems,* 340 pp., Prentice-Hall, Inc., Englewood Cliffs, N.J., 1974.

Lukas, R., E. Firing, P. Hacker, P. L. Richardson, C. A. Collins, R. Fine, and R. Gammon, Observations of the Mindanao Current during the Western Equatorial Pacific Ocean Circulation Study, *J. Geophys. Res., 96,* 7089-7104, 1991.

Maamaatuaiahutapu, K., V. C Garçon, C. Provost, M. Boulahdid, and A. P. Osiroff, Brazil-Malvinas confluence: Water mass composition, *J. Geophys. Res., 97,* 9493-9505, 1992.

Mackas, D. L., K. L. Denman, and A. F. Bennett, Least squares multiple tracer analysis of water mass composition, *J. Geophys. Res., 92,* 2907-2918, 1987.

Masumoto, Y., and T. Yamagata, Simulated seasonal circulation in the Indonesian seas, *J. Geophys. Res., 98,* 12,501-12,509, 1993.

Mc Gill, D. A., Light and nutrients in the Indian ocean, in *Ecological Studies, Analysis and Synthesis,* vol. 3, edited by B. Zeitzschel, pp. 53-102, Springer-Verlag, New York, 1973.

Metzl, N., B. Moore III, A. Papaud, and A. Poisson, Transport and carbon exchanges in Red Sea, Inverse methodology, *Global Biogeochem. Cycles, 3,* 1-26, 1989.

Metzl, N., B. Moore, and A. Poisson, Resolving the intermediate and deep advective flows in the Indian Ocean by using temperature, salinity, oxygen and phosphate data; the interplay of biogeochemical and geophysical tracers, *Palaeogeogr. Palaeoclimatol. Palaeoecol., 89,* 81-111, 1990.

Meyers, G., Variation of Indonesian throughflow and the El Nino – Southern Oscillation, *J. Geophys. Res., 101,* 12,255-12,263, 1996.

Miyama, T., T. Awaji, K. Akitomo, and N. Imasato, Study of seasonal transport variations in the Indonesian seas, *J. Geophys. Res., 100,* 20,517-20,541, 1995.

Molcard, R., M. Fieux, J. C. Swallow, A. G. Ilahude, and J. Banjarnahor, Low frequency variability of the currents in Indonesian channels (Savu-Roti and Roti-Ashmore Reef), *Deep Sea Res., Part I, 41,* 1643-1661, 1994.

Molcard, R., M. Fieux, and A.G. Ilahude, The Indo-Pacific throughflow in the Timor Passage, *J. Geophys. Res., 101,* 12,411-12,420, 1996.

Murray, S. P., and D. Arief, Throughflow into the Indian Ocean through the Lombok Strait, January 1985-January 1986, *Nature,* 333, 444-447, 1988.

Picaut, J., and T. Delcroix, Equatorial wave sequence associated with warm pool displacements during the 1986-1989 El Niño-La Niña, *J. Geophys. Res., 100,* 18,393-18,408, 1995.

Piola, A. R., and A. L. Gordon, Pacific and Indian ocean upper-layer salinity budget, *J Phys. Oceanogr., 14,* 747-753, 1984.

Quadfasel, D., A. Frische, and G. Cresswell, The circulation in the source area of the South Equatorial Current in the eastern Indian Ocean, *J. Geophys. Res., 101,* 12,483-12,488, 1996.

Redfield, A. C., The biological control of chemical factors in the environment, *Am. Sci., 46,* 205-222, 1958.

Rochford, D. J., Mixing trajectories of intermediate depth waters of the South-East Indian Ocean as determined by a salinity frequency method, *Aust. J. Mar. Freshwater Res., 14,* 1-23, 1963.

Rochford, D. J., Distribution of Banda Intermediate water in the Indian Ocean, *Aust. J. Mar. Freshwater Res., 17,* 61-76, 1966.

Rochford, D. J., Seasonal variations in the Indian ocean along 110°E, I, Hydrological structure of the upper 500m, *Aust. J. Mar. Freshwater Res., 20,* 1-50, 1969.

Schmitz, W. J , Jr., On the interbasin-scale thermohaline circulation., *Rev. Geophys., 33,* 151-173, 1995.

Takahashi, T., W. S. Broecker, and S. Langer, Redfield ratio based on chemical data from isopycnal surface, *J. Geophys. Res., 90,* 6907-6924, 1985.

Tomczak, M., A multi-parameter extension of temperature/salinity diagram techniques for the analysis of non-isopycnal mixing, *Prog. Oceanogr., 10,* 147-171, 1981.

Tomczak, M., and D. G. B. Large, Optimum multiparameter analysis of mixing in the thermocline of the eastern Indian Ocean, *J. Geophys. Res., 94,* 16,141-16,149, 1989.

Toole, J. M., and B. A. Warren, A hydrographic section across the subtropical South Indian Ocean, *Deep Sea Res., Part I, 40,* 1973-2019, 1993.

Treguer, P, and P. Le Corre, *Manuel d'analyse des Sels Nutritifs dans l'eau de Mer (Utilisation de l'autoAnalyser II Technicon®),* 2nd ed., 110 pp., Lab Oceanogr. Chim., Univ. de Bretagne Occidentale, Brest, France, 1975.

Van Aken, H. M., J Punjanan, and S. Saimma, Physical aspects of the flushing of the East Indonesian basins, *Neth. J. Sea Res., 22,* 315-340, 1988.

Van Bennekom, A. J., Deep water transit times in the eastern indonesian basins calculated from dissolved silica in deep and interstitial waters, *Neth. J. Sea Res., 22,* 341-354, 1988.

Warren, B. A., Transindian hydrographic section at Lat. 18°S: Property distributions and circulation in the South Indian Ocean, *Deep Sea Res., Part A, 28,* 759-788, 1981.

Wijffels, S , E. Firing, and J. Toole, The mean structure and variability of the Mindanao current at 8°N, *J. Geophys. Res., 100,* 18,421-18,435, 1995.

Wyrtki, K., Physical Oceanography of the Southeast Asian Waters, *Naga Rep., 2,* 195 pp, 1961.

Wyrtki, K , *Oceanographic Atlas of the International Indian Ocean Expedition,* 531 pp., Natl. Sci. Found., Washington, D. C., 1971.

You, Y., Seasonal variations of thermocline circulation and ventilation in the Indian Ocean, *J. Geophys. Res., 102,* 10,391-10,422, 1997.

You, Y., and M. Tomczak, Thermocline circulation and ventilation in the Indian Ocean derived from water mass analysis, *Deep Sea Res., Part I, 40,* 13-56, 1993.

C. Coatanoan, Department of Marine Chemistry and Geochemistry, Woods Hole Oceanographic Institution, 360 Woods Hole Road, MS 25, Woods Hole, MA 02543 (ccoatanoan@whoi.edu)

B. Coste, Laboratoire d'Océanographie et de Biogéochimie, CNRS, Centre d'Océanologie de Marseille, Case 901, 163 Avenue de Luminy, 13288 Marseille Cedex 09, France. (coste@com.univ-mrs.fr)

M. Fieux, Laboratoire d'Océanographie Dynamique et de Climatologie, CNRS/ORSTOM/UPMC, Université Paris 6, Case 100, 4 Place Jussieu, 75252 Paris Cedex 05, France (mf@lodyc.jussieu.fr)

N. Metzl, Laboratoire de Physique et Chimie Marines, INSU/ CNRS, Université Paris 6, Case 134, 4 Place Jussieu, 75252 Paris Cedex 05, France. (metzl@ccr.jussieu.fr)

(Received May 27, 1998, revised March 22, 1999;
accepted March 24, 1999)